HHS Public Access

Author manuscript

Cell Rep. Author manuscript; available in PMC 2021 September 06.

Published in final edited form as:

Cell Rep. 2021 August 17; 36(7): 109555. doi:10.1016/j.celrep.2021.109555.

Neuronal odor coding in the larval sensory cone of *Anopheles coluzzii:* Complex responses from a simple system

Huahua Sun[1,3], **Feng Liu**[1,3], **Adam P. Baker**[1], **H. Willi Honegger**[1], **Georg Raiser**[2], **Laurence J. Zwiebel**[1,4,*]

[1]Department of Biological Sciences, Vanderbilt University, 465 21st Avenue South, Nashville, TN 37235, USA

[2]Champalimaud Research, Avenida Brasília, Lisbon, Portugal

[3]These authors contributed equally

[4]Lead contact

SUMMARY

Anopheles mosquitoes are the sole vectors of malaria. Although adult females are directly responsible for disease transmission and accordingly have been extensively studied, the survival of pre-adult larval stages is vital. Mosquito larvae utilize a spectrum of chemosensory and other cues to navigate their aquatic habitats to avoid predators and search for food. Here we examine larval olfactory responses, in which the peripheral components are associated with the antennal sensory cone. Larval behavior and sensory cone responses to volatile stimuli in *Anopheles coluzzii* demonstrate the sensory cone is particularly tuned to alcohols, thiazoles, and heterocyclics, and these responses can be assigned to discrete groups of sensory cone neurons with distinctive profiles. These studies reveal that the anopheline larvae actively sample volatile odors above their aquatic habitats via a highly sophisticated olfactory system that is sensitive to a broad range of compounds with significant behavioral relevance.

In brief

Sun et al. investigate larval sensory cone and behavioral responses to volatile stimuli in *Anopheles coluzzii*. They find that malaria mosquito larvae actively sample volatile odors above their aquatic

*Correspondence: l.zwiebel@vanderbilt.edu.

AUTHOR CONTRIBUTIONS

H.S., F.L., H.W.H., and L.J.Z. designed the study. H.S. and F.L. performed experiments. H.S., F.L., A.P.B., and G.R. analyzed data and prepared the figures. H.S., F.L., A.P.B., H.W.H., G.R., and L.J.Z. interpreted the results and wrote the manuscript.

DECLARATION OF INTERESTS

The authors declare no competing interests.

SUPPORTING CITATIONS

The following references appear in the Supplemental information: Afify and Galizia (2014); Bentley et al. (1979, 1982); Comuzzo et al. (2006); Edwards et al. (1990); Leal et al. (2008); Li et al. (2009); Melo et al. (2020); Millar et al. (1992); Ponnusamy et al. (2008); Rinker et al. (2013); Silberbush et al. (2010); Varela et al. (2009); Waliwitiya et al. (2009).

SUPPLEMENTAL INFORMATION

Supplemental information can be found online at https://doi.org/10.1016/j.celrep.2021.109555.

habitats via a highly sophisticated olfactory system that is sensitive to a broad range of compounds with significant behavioral relevance.

Graphical Abstract

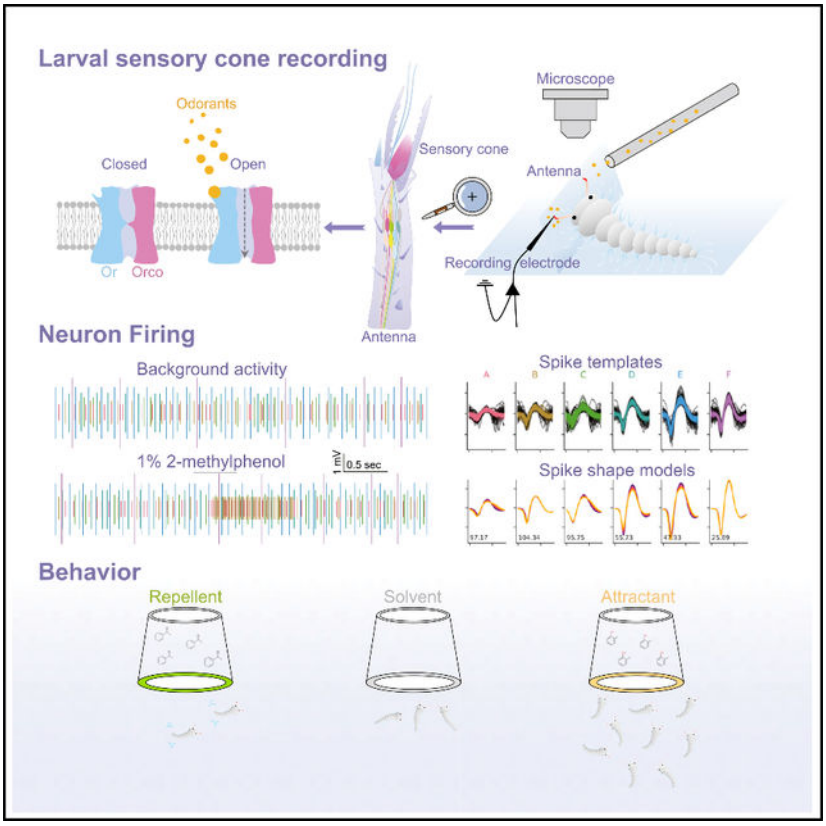

INTRODUCTION

Although significant progress has been made in advancing our understanding of the molecular and cellular basis of the olfactory system of adult mosquitoes (Lutz et al., 2017; Montell and Zwiebel, 2016; Zwiebel and Takken, 2004), considerably less is known about olfactory processes during the mosquito's pre-adult larval and pupal life stages where, paradoxically, the majority of successful malaria control strategies have been historically focused (Floore, 2006; Tusting et al., 2013). Anopheline larvae develop aquatically across four stages, known as instars, for approximately 10 days, depending on species and ambient temperature (Clements, 1992). Larval populations exist in restricted, often transient, and tenuous aqueous habitats, where they compete with each other in addition to a range of other life-forms, some of which are predatory, for food and survival. Rather than simply representing an immature life stage with relatively narrow perspectives, larval-stage mosquitoes are in fact highly complex, independent organisms that survive only by employing a wide range of physiological and sensory systems, with many of the same components and characteristics of similarly tasked adult processes. *Aedes aegypti* larvae are strongly attracted to fish food, extract of fish food, and RNA polynucleotides (Lutz et al.,

2019), as well as to proline and yeast, which also attract *Anopheles pseudopunctipennis* immatures (Gonzalez et al., 2019). Baker's yeast, which is a common component of laboratory rearing diets for mosquito larvae, has been reported to release up to 257 volatiles across 13 chemical groups (Alves et al., 2015), many of which have been used as odorants in this and other studies of mosquito larval chemosensory responses (Gonzalez et al., 2019; Merritt et al., 1992; Xia et al., 2008).

Although typically aquatic, anopheline larvae have also been found to display some amphibian characteristics, including egg hatching on damp soil in which larvae develop and even navigate terrestrially for limited periods of time over a short distance to surface water, where they complete their development (Miller et al., 2007; Koenraadt et al., 2003). During their fully aquatic stages, anopheline larvae display a range of behaviors, such as the acquisition of nutrients and avoidance of danger, and rely at least in part on their olfactory system to detect and respond to a complex set of chemical cues marking potential food sources (Xia et al., 2008), predators (Sih, 1986), and other aspects of their environment. Importantly, unlike aedine or culicine larvae, which dive to the bottom of their aquatic habitats to search for food, anopheline larvae mainly remain parallel to the surface, using their mouth brushes to filter potential food sources, such as microorganisms and other organic compounds (Fillinger et al., 2004; Gimnig et al., 2001). In this context, anopheline larvae are likely able to extend their antennae above the surface of their aquatic habitats to sample volatiles generated by the relatively high amounts of particulate and dissolved organic material (some of which act as larval nutrients), as well as a complex spectrum of microorganisms, many of which either directly constitute or emit volatile and non-volatile chemical cues. Some of these diverse compounds represent complex sets of semiochemicals that can attract and repel anopheline larvae (Danos et al., 1983; Wotton et al., 1997).

Mosquitoes and nearly all dipteran larvae share an array of homologous anterior appendages that comprise their principal chemosensory organs. The larval antennae extend distally from the head and include, at the apex, both a sensory cone and a peg organ that are respectively considered olfactory and gustatory organs (Lutz et al., 2017; Nicastro et al., 1998; Xia et al., 2008; Zacharuk et al., 1971). In *Drosophila melanogaster*, the larval olfactory apparatus consists of two bilaterally symmetrical dorsal organs, in which 21 odorant receptor (OR) neurons (ORNs) expressing 23 ORs, as well as Orco, the obligate co-receptor, have been identified (Kreher et al., 2005). In the dengue virus vector mosquito, *Ae. aegypti*, the larval sensory cone is innervated by 12–13 typical bipolar neurons expressing 24 *Or* genes, 15 of which are larvae specific (Bohbot et al., 2007; Zacharuk et al., 1971). Cellular and molecular studies of the *Anopheles coluzzii* and *Anopheles gambiae* (previously known as the "M" and "S" forms of the *An. gambiae* species complex) (Coetzee et al., 2013) larval olfactory apparatus, which comprise the antennae along with an apical sensory cone, have identified 12 putative chemosensory neurons that directly express OR/Orco receptor pairs, thereby implicating OR/Orco-based signaling (Liu et al., 2010; Xia et al., 2008). This is consistent with data reported here, in which *An. coluzzii orco*$^{-/-}$ mutant larvae are almost completely insensitive to volatile emanations from larval food (a mixture of yeast and fish food). In addition, several *An. coluzzii* variant ionotropic receptors (Irs), including the Ir8a, Ir25a, and Ir76b co-receptors, are expressed on the larval antennae, supporting the hypothesis that ORN- and ionotropic receptor neuron (IRN)-based chemosensory signaling represent two

distinct pathways involved in chemosensory-driven behaviors of anopheline larvae (Liu et al., 2010; Xia et al., 2008). These studies used aqueous-based bioassays to demonstrate that *An. coluzzii* larvae depend on their antennae and *orco* expression to respond behaviorally to a range of natural and synthetic odorants, such as cresol derivatives, 2-methylphenol, 3-methylphenol, and 4-methylcyclohexanol (Liu et al., 2010; Xia et al., 2008). Similarly, antennal ablations and RNAi-based silencing of both orco and the *An. gambiae Ir76b* co-receptor specifically altered Anopheles larval attraction to yeast and butylamine, respectively (Liu et al., 2010). Lastly, the functional characterization of several larval *Anopheles* ORs via heterologous expression in *Xenopus* oocytes shows that larval ORs respond to a range of odorants that have significant roles in larval chemical ecology (Xia et al., 2008).

Thus far, the characterization of *in vivo* electrophysiological responses of mosquito chemosensory neurons has been exclusively restricted to adult stages, with a limited number of studies restricted to terrestrial larvae in other insects (e.g., *Drosophila* and *Spodoptera* moths). Extracellular electrophysiological recordings from the dorsal organ in *Drosophila* revealed background firing from multiple ORNs with varying amplitudes, which proved difficult to fully sort but nevertheless uncovered several odorants that elicit excitatory neuronal responses, including 2-methylphenol, acetophenone, and benzaldehyde (Kreher et al., 2005). In addition, recordings from the caterpillar stages of *Spodoptera littoralis* moths revealed that its olfactory sensilla were sensitive to sex pheromone components and plant odors (Poivet et al., 2012; Rharrabe et al., 2014). In contrast, *in vivo* electrophysiological characterizations of larval olfactory responses have thus far not been reported in any mosquito, most likely because of the inherent challenges of the larval aquatic environment. This paucity of attention is paradoxical to the importance of mosquitoes as global disease vectors, as well as the central role that larval stages play in both the mosquito life cycle and historically effective control strategies. To address this knowledge gap, we have systematically characterized the olfactory responses of the *An. coluzzii* larval sensory cone using electrophysiological approaches adapted from adult single sensillum recording (SSR), and further demonstrate the behavioral responses of anopheline larvae to volatile compounds that elicit strong neuronal activation. Taken together, these studies illustrate that, as is true for adults, anopheline larvae have a complex and multi-faceted peripheral olfactory apparatus that provides a significant degree of chemosensory discrimination that is specifically adapted for the requirements of larval life.

RESULTS

Broad response profiles of the larval sensory cone of *An. coluzzii*

The larval antennae of mosquitoes encompass several orthologous structures that are morphologically conserved across individuals and instars. One of these structures, the sensory cone, which is approximately 5 μm in diameter (Figure S1A), is the site of peripheral chemosensory signal transduction for olfaction (Zacharuk et al., 1971). Although previous studies have catalogued and functionally analyzed the OR repertoire of the larval antennae *in vitro*, as well as the role of ORs and IRs in larval behavioral responses (Liu et al., 2010; Xia et al., 2008), we now report a comprehensive characterization of *in vivo* peripheral neuronal response profiles from the larval sensory cone in *An. coluzzii*. These

results provide a direct link between those responses and corresponding larval behaviors, as well as further illustrate the inherent complexity of the odor-coding paradigms of mosquito larvae. Initial electrophysiological surveys of the sensory cone on the tip of the larval antennae consistently revealed the presence of complex neuronal background activity (Figure S1C). Stimulus-independent action potential spikes from most recordings can be separated into several discrete groups based on their amplitudes (Figures S1 and S2), which confirms the presence of multiple neuronal dendrites within an individual larval sensory cone.

To investigate the broad olfactory profiles of *An. coluzzii* larvae, we initially examined collective (unsorted) neuronal responses after challenging the sensory cone with an in-house panel of 281 odorants, spanning 12 chemical classes that included aromatics, heterocyclics, alcohols, ketones, aldehydes, thiazoles, sulfurs, terpenoids, carboxylic acids, amines, esters, and others. Several of these compounds are components of larval food sources, predator emanations, and oviposition site volatiles (Figure 1A; Table S1) that have been shown previously to evoke behavioral activity in *An. coluzzii* larvae (Xia et al., 2008). Surprisingly, less than 20% of the 279 unitary odorants screened at 10^{-2} dilution elicited very strong olfactory responses (defined as ≥80 Δ spikes/s). Indeed, the frequency of robust (defined as 40–80 Δ spikes/s), modest (defined as 10–40 Δ spikes/s), and low responses (defined as <10 Δ spikes/s) was 29.1%, 41.6%, and 11.7%, respectively (Figure 1A; Table S2). Interestingly, the frequency of very strong excitatory responses was significantly higher among alcohols (67.9%), thiazoles (62.5%), and heterocyclics (38.1%) than terpenoids (4.8%) and esters (2.3%). Among the carboxylic acids, only hexanoic acid triggered robust responses (Figure 1A). A collective odorant-tuning curve spanning larval responses to all 281 odorants revealed a broad distribution with a very small kurtosis value (k = 0.136), which measures the peakedness of the distribution as a reflection of its generalization (Figure 1B) (Carey et al., 2010). Within the entire larval sensory cone tuning curve, it is very clear that alcohols, thiazoles, and heterocyclics with the strongest responses are clustered in the center, ketones with modest responses in the middle part of either side, while acids with the weakest response are observed at each end (Figure 1B). As expected, the apex responses were derived from three alcohols (1-pentanol, trans-3-hexen-1-ol, and 1-butanol) (Figure 1B). Taken together, these data suggest that the larval sensory cone is a generalist sensory appendage that displays a modest coding bias tuned toward alcohols, thiazoles, and to a somewhat lesser extent, heterocyclic-based cues.

Odorant tuning in the larval sensory cone is concentration-dependent

Our screening revealed a subset of 27 odorants that elicited strong responses from the *An. coluzzii* larval sensory cone. Within that subset, we addressed whether the sensory cone displayed dose-dependent responses, especially at low concentrations that are more likely to represent the natural environment of mosquito larvae. *An. coluzzii* larval sensory cone neurons were therefore interrogated using the robust response subpanel of 27 odorants at concentrations spanning five orders of magnitude (10^{-5} to 10^{-1} dilution; Figures 2A and 2C; Table S3). Most of the 27 odorants elicited a modest response at low concentration (10^{-4} and 10^{-5} dilutions). Furthermore, of those that did elicit a robust (≥40–80 Δ spikes/s) response at 10^{-2} dilution, only 13 maintained this intensity at lower (10^{-3})

dilutions (Figure 2A). A tuning curve analysis illustrates that these odorants evoke broad, concentration-dependent responses with characteristically low peakedness and are modestly biased toward 2,4,5-trimethylthiazole and 4-methylcyclohexanol at the lowest concentrations (10^{-5} and 10^{-4} dilutions, respectively), acetophenone at middle concentrations (10^{-2} and 10^{-3} dilutions), and butylamine at the highest concentration (10^{-1} dilution; Figure 2B). Across this range, sigmoidal dose-response curves showing clear saturation at 10^{-2} dilutions were observed for only two aromatics (2-ethylphenol, 2,4-dimethylphenol) and two ketones (cyclopentanone, acetophenone) (Figure 2C), further illustrating the larval sensory cone's response complexity. Interestingly, benzaldehyde elicited a general inhibition at 10^{-5} dilution but an increasing excitation between 10^{-3} and 10^{-1} dilutions (Figures 2A and 2C).

Diverse response patterns of the larval sensory cone to structurally similar odorants

We next sought to determine how mosquito larvae distinguish among odorants with similar molecular structures, and we repeatedly found them able to demonstrate strikingly different responses to each. For example, the strength of responses to carboxylic acids appeared to be highly dependent on carbon-chain length. Strong responses were elicited by hexanoic acid, but very weak responses were observed with shorter- and longer-chain acids (Figure 3A). Furthermore, the sensory cone strongly responded to aromatic/heterocyclic sulfurs, but aliphatic sulfurs elicited relatively weaker responses (Figure 3B). The location of alkane groups on a benzene ring may also be another discriminating factor. For example, responses between 2-ethylphenol and 4-ethylphenol or between 2,4-dimethylphenol and 2,5-dimethylphenol differed dramatically (Figure 3C). In addition, benzaldehyde-evoked responses significantly decreased when an extended alkane group was present on the benzene ring (Figure 3D). However, additional methyl groups on a thiazole ring increased the response strength when compared with a thiazole alone (Figure 3E). The mosquito larval sensory cone strongly responded to acetophenone, which is a known repellent of *An. coluzzii* larvae (Xia et al., 2008), although other stimuli with various side groups on the benzene ring of acetophenone exhibited a decreased response (Figure 3F). These data indicate that the neurophysiological responses of *An. coluzzii* larvae display a robust ability for detecting and discriminating complex chemical components, despite having only a small fraction of the neuronal and molecular repertoire present in the adult olfactory appendages.

Coding properties of neuronal groups in the larval sensory cone

To separate the response profiles of single units in the multiunit extracellular recordings, we computationally sorted larval cone spike trains into discrete neuronal groups using a novel spike sorting algorithm termed *SingleSensillumSort* (SSSort; see STAR Methods for a description). Using this approach, we sorted all recordings to the panel of 121 odorants that evoke supra-threshold responses at 10^{-2} odorant dilutions into six groups of larval chemosensory neurons (groups A–F, Figure 4A). All neuronal groups responded to multiple compounds, and all compounds evoked excitatory responses in at least one neuronal group. We also observed inhibitory responses in some of the neuron groups, most notably in groups D and E (Figure 4A), which may be the result of either direct odor-induced inhibition or ephaptic or lateral inhibition between neuron groups.

In general, alcohols made up the most potent chemical group, with several (e.g., 1-butanol, 1-pentanol, cis-3-hexenol, 3-methyl-1-butanol, and 3-methyl-2-buten-1-ol) evoking strong responses across all six neuronal groups. Several other unitary odorants dispersed across a subset of chemical groups were also found to activate all six neuron groups; these include 2-acetylpyridine, trans-2-pentenal, 2-methyl-2-thiazoline, and amyl acetate. Interestingly, different neuron groups displayed distinct tuning properties. For example, groups B and C were the most broadly tuned, groups E and F the most narrowly tuned, while groups A and D were more modestly tuned (Figure 4B). Further examination of the temporal dynamics of odorant responses across individual neuron groups using PST histogram analysis revealed that the neuronal responses to alcohols elicited phasic activation across neuron groups followed by pronounced inhibition (Figure S3). Most other aliphatic alcohols elicited a similar response pattern across all six neuronal groups. The unique temporal dynamics of alcohol-evoked larval sensory cone neurons may play a role in the feeding ecology of mosquito larvae, because alcohols are a major group of metabolic products of various bacteria.

To further investigate the temporal complexity of responses across the six neuron groups, we conducted a time-resolved sliding window covariance analysis on the firing rates from each group to every other one (Figure S4). Common change in firing rates between two units leads to positive covariances, while opposing changes in firing rate result in negative covariances (each row that would contain the covariance of a unit to itself is left blank in Figure S4). This analysis detects common or diverging changes in firing rate across units within a single trial. In response to (s)-1-octen-3-ol, for example, the firing rate of group B at first positively covaried with the rate from group C, although within 0.5 s after the onset of the odorant stimulation this relationship inverted. In addition to this biphasic response pattern in the temporal structure between groups B and C, a temporally segregated covariance pattern was observed in other groups. For example, group B showed positive covariance with groups D and F, while unit E showed a negative covariance with groups B and C that was sustained for a longer period. Therefore, the response to (s)-1-octen-3-ol is composed of at least an early and a late phase, with a distinct dynamic pattern of firing across neuronal groups, suggesting a complex temporal structure in the odor-specific neuronal coding initiating in the larval sensory cone of *An. coluzzii*.

To investigate the ability of the larval sensory cone to differentiate volatiles in the same chemical class, we examined the relationship among volatiles in an odor response space created by the responses of each neuronal group to the five major chemical classes. In this six-dimensional space, representing each neuronal group, the mean inter-odor Euclidean distances in spikes per second between all possible pairs within each chemical class were used to evaluate the capability of the larval sensory cone to distinguish those compounds. To visualize how compounds are distributed in this odor response space, we used principal-component analysis (PCA) to generate three-dimensional representations of the odor-response distributions in which the space between odor responses may be correlated to odor discrimination (Figures 5A–5E). Quantitative comparisons of the mean inter-odor Euclidean distance for each chemical class confirmed that alcohols are readily distinguishable (i.e., they display the largest inter-response distance), while esters seemed to be the most difficult to differentiate (i.e., the smallest distance; Figure 5F). Because

aromatic, ketone, and heterocyclic odorants are distinct from alcohols and esters, the capability of the larval sensory cone to discriminate among these groups appears to be limited (Figure 5F).

Anopheline larvae respond behaviorally to volatile odorants

As a correlate to our open-air electrophysiological analyses, we designed a simple laboratory-based behavioral preference bioassay to confirm that *An. coluzzii* larvae do indeed sample and respond to volatile odors in the headspace above their aquatic habitats. In this paradigm, free-swimming late instars are able to sample and respond behaviorally to a suite of unitary odorants that are presented solely as volatiles, in that the odorant sources in these assays are continuously maintained as physically separate from the larval water (Figure 6A). In these assays, we tested the behavioral response of anopheline larvae to larval food volatiles and to 24 odorants that elicited robust excitatory responses from the larval sensory cone. Unsurprisingly, volatiles emanating from larval food were robustly attractive to the larvae compared with water controls (Figure 6B). Moreover, mosquito larvae displayed significant attraction to multiple unitary odorants, such as 1-butanol, 3-hexanol, 3-octanol, 2-ethyl-1-hexanol, 2-methylphenol, 2-ethylphenol, pyridine, 2-acetylpyridine, and 2,4-dimethylbenzaldehyde (Figure 6B). Interestingly, volatiles emitted by 3-hexanol were also strongly attractive, while those of 1-hexanol, which is a straight-chain isomer of 3-hexanol, provoked robust larval aversion as was also elicited by acetophenone and 2,4,5-trimethylthiazole. Two of these compounds have previously been shown to elicit robust attraction (2-methylphenol) or aversion (acetophenone) in aqueous gradients present in the aquatic habitats of *Anopheles* larvae (Xia et al., 2008).

Orco-mediated neuronal and behavioral responses to volatiles

Previous work has established the critical role of the OR co-receptor (Orco) in the chemical ecology and OR-dependent olfactory responses of *An. coluzzii* larvae (Sun et al., 2020; Liu et al., 2010). To begin with, we examined the background neuronal activity across the larval sensory cone in *orco*$^{-/-}$ mutant larvae in which background activity, as well as the responses to 2-methylphenol and acetophenone and 72 other volatiles, were dramatically reduced relative to wild-type controls (Figures 7A and 7B) (Sun et al., 2020). To further determine the role of Orco in the neuronal and behavioral responses to these volatiles, we also utilized VUAA1, a highly specific Orco agonist (Jones et al., 2011) that can be volatized by heat (Ferguson et al., 2020; Yang et al., 2019; Pask et al., 2017), to challenge the larval sensory cone. As expected, volatile VUAA1 stimulation evoked robust neuronal firing broadly across the larval sensory cone (Figure 7C), which was largely abolished in the sensory cone of *orco*$^{-/-}$ mutant larvae (Figure 7D). Moreover, in contrast with wild-type larvae, the behavioral responses of *orco*$^{-/-}$ mutants to larval food, 2-methylphenol, 2-acetylpyridine, 1-butanol, 3-hexanol, and 2-ethyl-1-hexanol volatiles were significantly reduced, while responses to acetophenone and 1-hexanol were significantly increased (Figure 7E). These data further support the critical role of orco-mediated olfactory signaling in larval behavioral valence to semiochemicals in their environment. There was no significant difference between wild-type and *orco*$^{-/-}$ mutants in behavioral responses to 2-ethylphenol, pyridine, 2,4,5-trimethylthiazole, 3-octanol, and 2,4-dimethylbenzaldehyde

(Figure 7E), which supports the hypothesis that IR-mediated or other chemosensory pathways may be involved in the detection of those compounds.

DISCUSSION

In this study, we report a detailed electrophysiological investigation of larval peripheral olfactory responses and volatile-induced behavior to a broad set of volatile odorants in the Afrotropical malaria vector mosquito *An. coluzzii*. At first glance, and not surprisingly, when challenged by an odorant panel spanning a wide range of chemical space, distinct responses to a large number of compounds were observed (Figure 1; Table S2). Although one might reasonably question the hypothesis that *An. coluzzii* larvae sample volatiles above their aquatic habitats, it is noteworthy that, of the 26 compounds that are either fully miscible or have greater than 100 g/L aqueous solubility examined in this study (Table S1), only four (3-methyl-2-cyclohexenol, pyridine, 2-acetylpyridine, and 2,6-lutidine) elicited strong electrophysiological responses (>100 spike/s; Figure 1A; Table S2). Furthermore, although pyridine, 2-acetylpyridine, and 10 other odorants evoked strong neuronal excitation and elicited behavioral responses in volatile-based larval bioassays, several other compounds with a significant aqueous solubility were behaviorally inactive. These include cyclopentanone (60.8 g/L), 3-methyl-1-butanol (28 g/L), 1-pentanol (22 g/L), and 4-methylcyclohexanol (15 g/L; Figure 5). Conversely, of the 12 compounds that elicited significant larval attraction or repulsion and must therefore be considered to be semiochemicals, 7 had less than 6 g/L aqueous solubility. For example, acetophenone evoked consistent and robust aversive and attractive responses from *An. coluzzii* and *Ae. aegypti* larvae in direct (Gonzalez et al., 2015; Xia et al., 2008) and volatile (Figure 6) behavioral paradigms and also activated several larval OR/Orco complexes (Xia et al., 2008). Not surprisingly, acetophenone elicits extremely strong dose-dependent activation across the larval sensory cone (Figure 2) spanning across all six neuronal groups (Figure 4) and yet displays only modest aqueous solubility (5.5 g/L).

Two other compounds, 2,4,5-trimethylthiazole and 2-acetylpyridine, which had previously been shown to elicit the highest level of activation in heterologously expressed larval Or28 and strong activation of Or6, respectively (Xia et al., 2008), also displayed extremely strong dose-dependent activation of the larval sensory cone (Figure 2). That these highly active compounds have such different aqueous solubility (e.g., 2,4,5-trimethylthiazole: 0.53 g/L; 2-acetylpyridine: 134 g/L; Table S1) aligns nicely with the conclusion that the neuronal responses and significant repulsion and attraction displayed by anopheline larvae in response to these compounds are the result of stimuli volatized just above the aqueous surface of larval rearing cups (Figure 6). Interestingly, *An. gambiae* larvae were behaviorally indifferent to these compounds in a behavioral paradigm in which odorants were diffused into larval water from agarose plugs (Xia et al., 2008). This inconsistency likely reflects solubility and other considerations that lead to differential stimulus availability that is inherent in these behavioral paradigms.

In many natural habitats, anopheline larvae often reside in still water (Soleimani-Ahmadi et al., 2014; Amani et al., 2014) with organically abundant food sources, such as plant debris, rotten vegetables, and microorganisms (Sattler et al., 2005; Nilsson et al., 2018),

which are expected to release chemicals into the water and, importantly, emanate volatiles into the headspace immediately above, where they act as semiochemicals that can attract and repel anopheline larvae (Danos et al., 1983; Wotton et al., 1997). Several alcohols are byproducts of microbial metabolism or organic decay and act as larval food cues (Alves et al., 2015; Audrain et al., 2015; Beltran-Garcia et al., 1997). It is not surprising that alcohols occupy a good deal of the larval collective odor space, representing 56% of the odorants that elicit extremely strong neuronal responses (>100 spike/s) and that are more likely to be distinguishable than other chemical classes (Figure 5F). Of these, 1-hexanol is a robust volatile larval repellent, while 1-butanol, 3-octanol, and 2-ethyl-1-hexanol volatiles induce larval attraction (Figure 6).

As previously noted, the link between peripheral olfactory sensitivity and larval behavior is obvious, although not straightforward (Xia et al., 2008). Indeed, the robust complexity of olfactory sensitivity displayed by *An. coluzzii* larvae is further illustrated by an examination of concentration dependency (Figure 2; Table S3). Although every odorant in the panel elicited dose-dependent responses across 5 orders of magnitude dilutions, several compounds (e.g., 1-octen-3-ol, acetophenone, cyclopentanone, 2-ethylphenol) exhibited saturation kinetics at the highest (10^{-1}) odorant dilutions. Larval responses to butylamine are notable in terms of intensity and near-exponential kinetics. A survey of odorant tuning curves across several dilutions confirms that the *An. coluzzii* larval sensory cone maintains a generalist sensitivity to environmental cues while displaying robust sensitivity to several behaviorally active compounds. These include butylamine, which evokes dose-dependent effects on *An. coluzzii* larval movements (Liu et al., 2010; Xia et al., 2008); acetophenone, which evokes significant aversive behavior when present in larval water (at the dilution as low as 10^{-5}; Xia et al., 2008), as well as volatized above the water surface (at the dilution of 10^{-3}, this study); and 4-methylcyclohexanol, which is most attractive to *An. coluzzii* larvae when dissolved in the water at 10^{-4} dilution (Sih, 1986; Xia et al., 2008) and just above the water surface at 10^{-3} dilution (this study). It is noteworthy that these odorants evoked larval behavioral effects that closely mirror their sensory cone response ranges (Figures 2A and 2C) and their tuning-curve peak prominence across much of that spectrum (Figure 2B). The alignments between larval peripheral neuronal activity and behavior serve to underscore the close relationship between electrophysiological and behavioral responses.

Despite limitations in precisely discriminating the action potential spikes from individual discrete chemosensory neurons that innervate the larval sensory cone, a computational approach was taken to sort complex spike trains into six distinct neuronal classes. In addition to sensory cone spike amplitude, which reflects cell body morphology and relative location (Sih, 1986; Xia et al., 2008), this approach took spike shape parameters into account and, importantly, analyzed how shape parameters vary as a function of the neuron's firing rate (Figure S2). Resolving these collective neuronal responses into six clusters of sensory neurons further illustrated the dynamic complexity of the larval olfactory system of *An. coluzzii* by revealing temporally structured responses that might be of functional significance for odor coding (Figure S4). Although the breadth and intensity of the A, B, and C group responses (displaying relatively small spike amplitudes) are more prominent than in D, E, and F group neurons (which possess relatively large spike amplitudes), there are nevertheless numerous odorants that preferentially activate or inhibit D, E, and F group

neurons. These include anisole, isobutyl acetate, and indole, which are metabolic byproducts of bacteria (Elgaali et al., 2002; Hubbard et al., 2015; Lindh et al., 2008; Schulz and Dickschat, 2007), fungi (Chen et al., 2014; Tomberlin et al., 2017), and plants (Frey et al., 2000; Ober, 2005; Turlings et al., 1991). It is therefore reasonable to speculate that mosquito larvae might use indole as an olfactory cue to locate potential food sources. Indeed, it has been shown to be a potent attractant for anopheline larvae and specifically recognized by Or2 and Or10, both of which are expressed in the larval antennae (Xia et al., 2008). Lastly, the inhibitory responses to several volatiles uncovered by *orco*$^{-/-}$ mutant sensory cones (Sun et al., 2020) and the inhibition of background spiking, as well as the relative sparsity of excitatory responses characteristic of D, E, and F group neurons reported here, may, in part, reflect the impact of ephaptic interactions between neurons (Figure 4) within the closely packed chemosensory neurons of the larval antennae, as has been observed in *Drosophila* ORNs (Su et al., 2012).

Although larval ORs have been identified and, in many cases, localized to specific ORNs (Xia et al., 2008) and also have been functionally characterized (Carey et al., 2010; Wang et al., 2010; Xia et al., 2008), in the absence of a suite of overlapping tuning *Or* gene-targeting mutants, it is not possible to precisely map responses to discrete ORs. Although those studies identified several larval ORs with relatively narrow tuning breadths, the data also reveal that many odorants seem to activate multiple receptors almost promiscuously. In addition to ORs, the larval antennae of *An. coluzzii* expressed a set of functional IRs that include the full suite of Ir8a, Ir25a, and Ir76b co-receptors, the latter of which has been specifically implicated in aqueous-based and antennal-dependent behavioral responses of larvae to butylamine (Liu et al., 2010). In that light, it is likely that the robust dose-dependent responses of the larval sensory cone to butylamine, pentylamine, isopentylamine, and other amines are the result of IR-based signaling. In addition, while IR-based signaling has been directly implicated in responses to volatile acid-based semiochemicals in adult *Ae. aegypti* (Raji et al., 2019) and *Drosophila* (Ai et al., 2010), it is interesting that, with the sole exception of distinct sensitivity to hexanoic acid, the larval sensory cone *of An. coluzzii* was largely indifferent to acidic volatiles (Figures 1 and 3). Although recent studies have established that IR- and OR-linked pathways are co-expressed and functional in a subset of *Ae. aegypti* and *Drosophila* adult chemosensory neurons (Task et al., 2020; Younger et al., 2020), we have not examined that possibility. Instead, and without excluding that possibility, we favor a model in which a significant component of larval antennal responses to amines and acids are largely dependent on IR-based signaling resident in the sensory cone and sensory peg, respectively.

The studies reported here demonstrate that anopheline larval olfactory physiology displays intricate dose-dependent and richly discriminatory response profiles. Taken together, the data presented here reinforce the premise that anopheline larvae are complex aquatic insects that benefit from the presence of a versatile olfactory apparatus through which they can sense environmental volatiles. The sensory cone and peg together with perhaps other components of the larval antennae provide anophelines with a robust capacity to navigate and detect a wide range of chemical cues to locate and select nutrients, as well as identify predators and other signals they may encounter in their aquatic habitats, doubtlessly promoting larval survival and maturation to adults. In contrast with the 1,000+

chemosensory neurons that constitute the adult olfactory system, larval mosquitoes are comprised of a relatively simple and more accessible neuronal apparatus that allows study of odor coding and neuronal function and, importantly, presents a viable target for the design of novel control strategies that could be applied to their relatively restricted aquatic habitats to reduce their potential to develop into adult disease vectors.

STAR★METHODS

RESOURCE AVAILABILITY

Lead contact—Further information and requests for resources and reagents should be directed to and will be fulfilled by the Lead Contact, L.J. Zwiebel (l.zwiebel@vanderbilt.edu).

Materials availability—This study did not generate new unique reagents.

Data and code availability—The published article includes all data generated during the study and the raw data are available upon request from the Lead Contact. Any additional information required to reanalyze the data reported in this paper is available from the lead contact upon request.

EXPERIMENTAL MODEL AND SUBJECT DETAILS

Animals and housing—*An. coluzzii* adults were reared at 27°C, 75% humidity under a 12 h light/12 h dark photoperiod and supplied with 10% sucrose water in the Vanderbilt University Insectary (Fox et al., 2001; Suh et al., 2016). For stock propagation, 5- to 7-day-old mated females were blood-fed for 30–45 min using a membrane feeding system (Hemotek, Lancaster, UK) filled with defibrinated sheep blood purchased from Hemostat Laboratories (Dixon, CA, USA).

Mosquito larvae were reared in distilled water at 27°C under the standard 12 h light/12 h dark cycle, with approximately 300 larvae per rearing pan in 1 L H_2O. The larval food was made from 0.12 g/mL Kaytee Koi's Choice premium fish food (Chilton, WI, US) plus 0.06 g/mL yeast in distilled water and subsequently incubated at 4°C overnight for fermentation. For first and second instar larvae, 0.08 mL larval food was added into the water every 24 h. For third and fourth instar larvae, 1 mL larval food was added.

METHOD DETAILS

Electrophysiology—Inasmuch as Anopheline larvae have been shown to briefly maintain terrestrial habitats and thereafter spend considerable periods of time at the surface of their aquatic habitats where we hypothesize they extend their antennae above their aqueous environments to sample volatile odorants (Koenraadt et al., 2003), we examined peripheral responses to volatile stimuli on the larval antennal sensory cone. To accomplish this, electrophysiological recordings of the *An. coluzzii* larval antennal sensory cone were conducted in the air using an adaptation of the well-established SSR technique (Sun et al., 2020; Liu et al., 2013). Here, 3rd instar larvae selected based on large body size and aggressive activity (Xia et al., 2008; Liu et al., 2010) were hand transferred via their

abdomen with fine forceps (#5 Dumont, Switzerland) from rearing pans to KimWipes (Kimberly Clark, Fisher Scientific) for 30 s to remove excess liquid while avoiding rolling or otherwise damaging the antennae. After drying, individual larvae were hand transferred and mounted on 76 × 26-mm microscope slides. The dorsal surface of the larval antennae was attached to a coverslip using double-sided tape, and an insect pin was used to press the larval head onto the tape to prevent its further movement. The coverslip was placed on a small bead of dental wax acting as a pivot point, which facilitates manipulation so the coverslip could be placed at approximately 60–90 degrees relative to the head (Figure S1B).

Once mounted, the specimen was positioned onto the stage of an Olympus BX51WI microscope, and its antennae and sensory cone were visualized at high (1000 ×) and moderate (200 ×) magnification to confirm the placement of the entire preparation. Tungsten microelectrodes (sharpened in 10% KNO_2 at 10 V) were used for both the grounded reference electrode (inserted into the larval compound eye using a micromanipulator (World Precision Instruments, Sarasota, FL) and the recording electrode (inserted into the base of the antennal sensory cone) to complete the electrical circuit to extracellularly record olfactory sensory neuron (OSN) potentials (Den Otter et al., 1980) (Figure S1A). Multiple placements for the recording electrode along the antennal sensory cone were initially examined during the development of our recording preparation, each of which was found to provide nearly identical visualization of spontaneous (non-stimulus associated) neuronal activity (Figure S1C). That said, positioning of the recording electrode at the base of the sensory cone was used throughout this study as it provided optimal stability and was the most favored path for an implementation having the most straightforward approach in our microscope setup. As is frequently observed in SSR studies in adult mosquitoes, the depth of electrode insertion into the sensory cone influences the signal-noise ratio. To optimize and provide uniformity for placement of the recording electrode, the depth was adjusted using a piezoelectric micromanipulator (Model PCS6000, Burleigh EXFO Life Sciences, Ontario, Canada) to provide a very clean baseline. The pre-amplifier was connected to an analog-to-digital signal converter (IDAC-4, Syntech, the Netherlands) at a sample rate of 96,000 samples per second and 10 × amplification, which in turn was connected to a PC for signal recording and offline analysis. Controlled manipulation of the recording electrode was performed using a Burleigh micromanipulator (Model PCS6000). All electrodes were connected to a pre-amplifier (Syntech universal AC/DC 10 ×, Syntech, Hilversum, the Netherlands) and from there to an analog-to-digital signal converter (IDAC-4, Syntech, Hilversum, the Netherlands) at a sample rate of 96,000 samples per second and 10 × amplification, which in turn was connected to a dedicated PC for signal recording and offline analysis.

Odorant preparation and stimulus application—Compounds of the highest purity, typically ≥ 99% (Sigma-Aldrich), were diluted in paraffin oil, dimethyl sulfoxide (DMSO), or diethyl pyrocarbonate (DEPC)-treated ddH_2O to make v/v (for liquids) or m/v (for solids) solutions at specified concentrations. For each compound, a 10 μL portion was dispersed onto filter paper (3 × 10 mm), which was then inserted into a Pasteur pipette to create the stimulus cartridge. A sample containing the solvent alone served as the control. The airflow across the antennae was maintained at a constant 20 mL/s throughout the experiment.

Purified and humidified air was delivered to the preparation through a glass tube (10-mm inner diameter) perforated by a small hole 10-cm away from the end of the tube into which the tip of the Pasteur pipette could be inserted. The stimulus was delivered to the larval sensory cone by inserting the tip of the stimulus cartridge into this hole and diverting a portion of the air stream (0.5 L/min) to flow through the stimulus cartridge for 500 ms (0.5 s) using a Syntech stimulus controller CS-55 (Syntech, Hilversum, the Netherlands). The distance between the end of the glass tube and the antennae was ≤ 1 cm. For dose-response relationships, serial ten-fold dilutions were used to challenge the larval sensory cone, starting from solvent control, and thereafter proceeding from highest dilutions/lowest doses to lowest dilutions/highest doses with at least 60 s intervals between odor stimulations. During preliminary recordings, robust neuronal activities from the sensory cone under these conditions were observed for at least 1 h. Nevertheless, individual sensory cone SSR preparations in this study were used for a maximum of thirty stimulations conducted over no more than 30 min while continually monitoring for fading or disruption of background neuronal activity. Stimuli signals were recorded for 10 s, starting 2 s before stimulation, and the background action potentials from the entire sensory cone were counted offline over one 500-ms period before the stimulus and over four 500-ms periods during and after stimulation. Spike rates observed during the 500-ms stimulation/post-stimulation windows were normalized by subtracting the pre-stimulus (background) activities observed in the preceding 500 ms, with counts recorded in units of spikes/s. Lastly, odorant responses, described as Δspikes/s, were normalized by subtracting the solvent responses in each individual recording.

Spike sorting—SSRs pose a challenge to spike sorting algorithms because the voltage signals of recorded neurons not only all overlap on a single recording site, but also, and in particular, because the individual neuron spike shapes change as a function of the neuronal firing rate. While most spike sorting algorithms employ some form of pattern recognition (such as template matching) to assign spikes to units, any changes in spike shape degrade the sorting quality. To address this, we have developed a novel spike sorting algorithm SingleSensillumSort (SSSort) that explicitly builds a model of how the temporal shape of each neuron's spikes changes as a function of its own firing rate, and then uses these models to assign the best matching unit for a given spike. SSSort is a generalization and extension of SeqPeelSort (Raiser, 2018) with respect to arbitrary spike shape changes, via forming an explicit model of how these changes depend on firing rate.

In brief, SSSort first detects all spikes in a recording and extracts the waveform shape around a temporal window. On these spike templates, k-means clustering is used to seed the algorithm with an initial set of unit identities. Based on the morphology of the sensory cone (Xia et al., 2008), we chose this initial seed to be k = 12. This assigns each spike to a unit, making it possible to estimate the unit's firing rates at the time of each spike occurrence, which, in turn, allows the algorithm to construct an explicit model on how the spike shape changes as a function of the firing rate. Using these models, each spike in the recording is then compared with a predicted spike shape of each unit at its current firing rate, and the spike is assigned to the best matching unit. This is repeated in an iterative manner, such that upon each iteration, new and better models are formed. Furthermore, the

pairwise Euclidean distances between all spikes assigned to a given unit are compared with the pairwise Euclidean distance across units, and two units are merged if the across distance is lower than the within distance.

The SSSort algorithm was allowed to run until scores stabilized, typically yielding between 8 and 11 units. Spike clusters were then manually excluded based on three criteria: whether (1) the extracted templates exhibited malformed shapes that were unlikely to be physiological spikes (such as double peaks); (2) spike amplitudes were too close to the noise floor to be sorted reliably; or (3) units showed no baseline firing rate and always only spiked after stimulation. In this case, we assumed that these spikes represent instances in which the algorithm failed to assign strongly deformed spikes to any other unit, and accordingly they were excluded from further analysis. The remaining six units were denoted as A-F and sorted by their ascending spike amplitude. Inasmuch as we cannot strictly state that a single neuron in any class is the same neuron across replicate recordings, these assemblies are termed neuron groups rather than single units. An in-depth description of the algorithm, its parameters, and all source code can be found at https://github.com/grg2rsr/SSSort. A graphical representation of the algorithm's function and performance is provided in Figure S2.

Free swimming larval preference behavioral bioassay—One hundred *An. coluzzii* second or third instar larvae were collected, gently rinsed, and maintained at 27°C in dH_2O without food for 2 h. Odorant dilutions (10^{-3} v/v or w/v) were prepared in DMSO. Attraction/repulsion behavioral bioassays were performed in an open Pyrex dish (38.1 × 25.4 × 5.08 cm) arena filled with 1000 mL of 27°C dH_2O, set up in a temperature-controlled walk-in environmental rearing chamber also maintained at 27°C. Food-deprived larvae were initially released in the center of the dish and allowed to swim freely for 30 min to acclimate to the arena. Volatile stimulus chambers were fabricated using 5.5-oz plastic cups (AV. Inc, Model 8541948156) with 3-cm diameter holes cut into their 5-cm diameter covers. Floating chambers were inverted, placed on the surface of the larval rearing water, and held in place at opposite ends of the behavioral arena. To initiate each trial, 500 μL of diluted odorant or solvent was transferred to the inner side of the cup lids (which remained out of contact with the larval rearing water) to provide a volatile odor (treatment) or solvent (control) stimuli within each inverted cup stimulus chamber. Mosquito larvae were thereafter allowed to swim freely in the arena between the treatment or control cups for 1 h, at which point the number of larvae directly under each cup was manually quantified. Sham negative control assays (n = 8) with DMSO solvent in both cups were regularly conducted during each trial. Behavioral preference index (PI) was calculated as follows: PI = (#odorant − #solvent control)/(#odor + #control), where the #odorant indicates the number of larvae directly under the odorant-containing treatment cup and the #control indicates the number of larvae present under the solvent-alone control cup. Respective PI values for each compound were compared with those of sham assays and assessed for statistical significance using unpaired, two-tailed Student's t tests with Welch's correction with GraphPad Prism software.

QUANTIFICATION AND STATISTICAL ANALYSIS

Depending upon the data generated, an ANOVA or a t test has been used. The figure legends note the statistical tests used, the n values, P values and SEMs. Method details also contain the type of statistical test used.

Supplementary Material

Refer to Web version on PubMed Central for supplementary material.

ACKNOWLEDGMENTS

We gratefully acknowledge helpful critiques from anonymous reviewers and thank Drs. Christopher Potter (Johns Hopkins School of Medicine), Ann Carr, Stephen Ferguson, and Zi Ye for their comments on this manuscript, as well as other members of the Zwiebel lab for critical suggestions and help with data analyses. We also thank Dr. Yuan Yuan (Michigan State University) for advice on spike sorting and Dr. A.M. McAinsh for editorial assistance, as well as Zhen Li and Samuel Ochieng for mosquito rearing and technical help. This work was conducted with the support of Vanderbilt University and a grant from the National Institutes of Health (NIAID; AI127693 to L.J.Z.).

REFERENCES

Afify A, and Galizia CG (2014). Gravid females of the mosquito *Aedes aegypti* avoid oviposition on m-cresol in the presence of the deterrent isomer p-cresol. Parasit. Vectors 7, 315. [PubMed: 25008201]

Ai M, Min S, Grosjean Y, Leblanc C, Bell R, Benton R, and Suh GS (2010). Acid sensing by the *Drosophila* olfactory system. Nature 468, 691–695. [PubMed: 21085119]

Alves Z, Melo A, Figueiredo AR, Coimbra MA, Gomes AC, and Rocha SM (2015). Exploring the *Saccharomyces cerevisiae* volatile metabolome: Indigenous versus commercial strains. PLoS ONE 10, e0143641. [PubMed: 26600152]

Amani H, Yaghoobi-Ershadi MR, and Kassiri H (2014). The ecology and larval habitats characteristics of anopheline mosquitoes (Diptera: Culicidae) in Aligudarz County (Luristan province, western Iran). Asian Pac. J. Trop. Biomed. 4 (Suppl 1), S233–S241. [PubMed: 25183088]

Audrain B, Farag MA, Ryu CM, and Ghigo JM (2015). Role of bacterial volatile compounds in bacterial biology. FEMS Microbiol. Rev. 39, 222–233. [PubMed: 25725014]

Beltran-Garcia MJ, Estarron-Espinosa M, and Ogura T (1997). Volatile Compounds Secreted by the Oyster Mushroom (*Pleurotus ostreatus*) and Their Antibacterial Activities. J. Agric. Food Chem. 45, 4049–4052.

Bentley MD, McDaniel IN, Yatagai M, Lee HP, and Maynard R (1979). p-Cresol: an oviposition attractant of *Aedes triseriatus*. Environ. Entomol. 8, 206–209.

Bentley MD, McDaniel IN, and Davis EE (1982). Studies of 4-methylcyclohexanol: an *Aedes triseriatus* (Diptera: Culicidae) oviposition attractant. J. Med. Entomol. 19, 589–592. [PubMed: 7143381]

Bohbot J, Pitts RJ, Kwon HW, Rützler M, Robertson HM, and Zwiebel LJ (2007). Molecular characterization of the *Aedes aegypti* odorant receptor gene family. Insect Mol. Biol. 16, 525–537. [PubMed: 17635615]

Carey AF, Wang G, Su CY, Zwiebel LJ, and Carlson JR (2010). Odorant reception in the malaria mosquito *Anopheles gambiae*. Nature 464, 66–71. [PubMed: 20130575]

Chen G, Zhang RR, Liu Y, and Sun WB (2014). Spore dispersal of fetid *Lysurus mokusin* by feces of mycophagous insects. J. Chem. Ecol. 40, 893–899. [PubMed: 25064696]

Clements AN (1992). Chapter 2: Larval Nutrition, Excretion and Respiration. The Biology of Mosquitoes, Volume 1: Development, Nutrition and Reproduction (CABI Publishing), pp. 231–234.

Coetzee M, Hunt RH, Wilkerson R, Della Torre A, Coulibaly MB, and Besansky NJ (2013). *Anopheles coluzzii* and *Anopheles amharicus*, new members of the Anopheles gambiae complex. Zootaxa 3619, 246–274. [PubMed: 26131476]

Comuzzo P, Tat L, Tonizzo A, and Battistutta F (2006). Yeast derivatives (extracts and autolysates) in winemaking: Release of volatile compounds and effects on wine aroma volatility. Food Chem. 99, 217–230.

Danos SC, Maki JS, and Remsen CC (1983). Stratification of microorganisms and nutrients in the surface microlayer of small freshwater ponds. Hydrobiologia 98, 193–202.

Den Otter CJ, Behan M, and Maes FW (1980). Single cell responses in female *Pieris brassicae* (Lepidoptera: Pieridae) to plant volatiles and conspecific egg odours. J. Insect Physiol. 26, 465–472.

Edwards CG, Beelman R, Bartley C, and McConnell A (1990). Production of decanoic acid and other volatile compounds and the growth of yeast and malolactic bacteria during vinification. Am. J. Enol. Vitic. 41, 48–56.

Elgaali H, Hamilton-Kemp TR, Newman MC, Collins RW, Yu K, and Archbold DD (2002). Comparison of long-chain alcohols and other volatile compounds emitted from food-borne and related Gram positive and Gram negative bacteria. J. Basic Microbiol. 42, 373–380. [PubMed: 12442299]

Ferguson ST, Park KY, Ruff AA, Bakis I, and Zwiebel LJ (2020). Odor coding of nestmate recognition in the eusocial ant *Camponotus floridanus*. J. Exp. Biol. 223, jeb215400. [PubMed: 31900348]

Fillinger U, Sonye G, Killeen GF, Knols BGJ, and Becker N (2004). The practical importance of permanent and semipermanent habitats for controlling aquatic stages of Anopheles *gambiae sensu lato* mosquitoes: operational observations from a rural town in western Kenya. Trop. Med. Int. Health 9, 1274–1289. [PubMed: 15598259]

Floore TG (2006). Mosquito larval control practices: past and present. J. Am. Mosq. Control Assoc. 22, 527–533. [PubMed: 17067057]

Fox AN, Pitts RJ, Robertson HM, Carlson JR, and Zwiebel LJ (2001). Candidate odorant receptors from the malaria vector mosquito *Anopheles gambiae* and evidence of down-regulation in response to blood feeding. Proc. Natl. Acad. Sci. USA 98, 14693–14697. [PubMed: 11724964]

Frey M, Stettner C, Paré PW, Schmelz EA, Tumlinson JH, and Gierl A (2000). An herbivore elicitor activates the gene for indole emission in maize. Proc. Natl. Acad. Sci. USA 97, 14801–14806. [PubMed: 11106389]

Gimnig JE, Ombok M, Kamau L, and Hawley WA (2001). Characteristics of larval anopheline (Diptera: Culicidae) habitats in Western Kenya. J. Med. Entomol. 38, 282–288. [PubMed: 11296836]

Gonzalez PV, Alvarez Costa A, Harburguer LV, and Masuh HM (2019). Quantitative evaluation of the behavioral response to attractant and repellent compounds in *Anopheles pseudopunctipennis* and *Aedes aegypti* (Diptera: Culicidae) larvae. J. Econ. Entomol. 112, 1388–1395. [PubMed: 30753516]

Gonzalez, Paula V, Audino González, Paola A, and Masuh, Héctor M (2015). Behavioral response of *Aedes aegypti* (Diptera: Culicidae) larvae to synthetic and natural attractants and repellents. J. Med. Entomol. 52, 1315–1321. [PubMed: 26352935]

Hubbard TD, Murray IA, and Perdew GH (2015). Special section on drug metabolism and the microbiome-Minireview indole and tryptophan metabolism: Endogenous and dietary routes to ah receptor activation. Drug Metab.Dispos. 43, 1522–1535. [PubMed: 26041783]

Jones PL, Pask GM, Rinker DC, and Zwiebel LJ (2011). Functional agonism of insect odorant receptor ion channels. Proc. Natl. Acad. Sci. USA 108, 8821–8825. [PubMed: 21555561]

Koenraadt CJ, Paaijmans KP, Githeko AK, Knols BG, and Takken W (2003). Egg hatching, larval movement and larval survival of the malaria vector *Anopheles gambiae* in desiccating habitats. Malar. J. 2, 20. [PubMed: 12919636]

Kreher SA, Kwon JY, and Carlson JR (2005). The molecular basis of odor coding in the *Drosophila* larva. Neuron 46, 445–456. [PubMed: 15882644]

Leal WS, Barbosa RM, Xu W, Ishida Y, Syed Z, Latte N, Chen AM, Morgan TI, Cornel AJ, and Furtado A (2008). Reverse and conventional chemical ecology approaches for the development of oviposition attractants for Culex mosquitoes. PLoS ONE 3, e3045. [PubMed: 18725946]

Li J, Deng T, Li H, Chen L, and Mo J (2009). Effects of water color and chemical compounds on the oviposition behavior of gravid *Culex pipiens pallens* females under laboratory conditions. J. Agric. Urban Entomol. 26, 23–30.

Lindh JM, Kännaste A, Knols BGJ, Faye I, and Borg-Karlson AK (2008). Oviposition responses of *Anopheles gambiae* s.s. (Diptera: Culicidae) and identification of volatiles from bacteria-containing solutions. J. Med. Entomol. 45, 1039–1049. [PubMed: 19058627]

Liu C, Pitts RJ, Bohbot JD, Jones PL, Wang G, and Zwiebel LJ (2010). Distinct olfactory signaling mechanisms in the malaria vector mosquito *Anopheles gambiae*. PLoS Biol. 8, e1000467. [PubMed: 20824161]

Liu F, Chen L, Appel AG, and Liu N (2013). Olfactory responses of the antennal trichoid sensilla to chemical repellents in the mosquito, *Culex quinquefasciatus*. J. Insect Physiol. 59, 1169–1177. [PubMed: 24035746]

Lutz EK, Lahondère C, Vinauger C, and Riffell JA (2017). Olfactory learning and chemical ecology of olfaction in disease vector mosquitoes: a life history perspective. Curr. Opin. Insect Sci. 20, 75–83. [PubMed: 28602240]

Lutz EK, Grewal TS, and Riffell JA (2019). Computational and experimental insights into the chemosensory navigation of *Aedes aegypti* mosquito larvae. Proc. Biol. Sci. 286, 20191495. [PubMed: 31744443]

Melo N, Wolff GH, Costa-da-Silva AL, Arribas R, Triana MF, Gugger M, Riffell JA, DeGennaro M, and Stensmyr MC (2020). Geosmin attracts *Aedes aegypti* mosquitoes to oviposition sites. Curr. Biol. 30, 127–134.e5. [PubMed: 31839454]

Merritt RW, Dadd RH, and Walker ED (1992). Feeding behavior, natural food, and nutritional relationships of larval mosquitoes. Annu. Rev. Entomol. 37, 349–376. [PubMed: 1347208]

Millar JG, Chaney JD, and Mulla MS (1992). Identification of oviposition attractants for *Culex quinquefasciatus* from fermented Bermuda grass infusions. J. Am. Mosq. Control Assoc. 8, 11–17. [PubMed: 1583482]

Miller JR, Huang J, Vulule J, and Walker ED (2007). Life on the edge: African malaria mosquito (*Anopheles gambiae s. l.*) larvae are amphibious. Naturwissenschaften 94, 195–199. [PubMed: 17139499]

Montell C, and Zwiebel LJ (2016). Mosquito sensory systems. Adv. Insect Physiol. 51, 293–328.

Nicastro D, Melzer RR, Hruschka H, and Smola U (1998). Evolution of small sense organs: Sensilla on the larval antennae traced back to the origin of the diptera. Naturwissenschaften 85, 501–505.

Nilsson LKJ, Sharma A, Bhatnagar RK, Bertilsson S, and Terenius O (2018). Presence of *Aedes* and *Anopheles* mosquito larvae is correlated to bacteria found in domestic water-storage containers. FEMS Microbiol. Ecol. 94, fiy058.

Ober D (2005). Seeing double: gene duplication and diversification in plant secondary metabolism. Trends Plant Sci. 10, 444–449. [PubMed: 16054418]

Pask GM, Slone JD, Millar JG, Das P, Moreira JA, Zhou X, Bello J, Berger SL, Bonasio R, Desplan C, et al. (2017). Specialized odorant receptors in social insects that detect cuticular hydrocarbon cues and candidate pheromones. Nat. Commun. 8, 297. [PubMed: 28819196]

Poivet E, Rharrabe K, Monsempes C, Glaser N, Rochat D, Renou M, Marion-Poll F, and Jacquin-Joly E (2012). The use of the sex pheromone as an evolutionary solution to food source selection in caterpillars. Nat. Commun. 3, 1047. [PubMed: 22948829]

Ponnusamy L, Xu N, Nojima S, Wesson DM, Schal C, and Apperson CS (2008). Identification of bacteria and bacteria-associated chemical cues that mediate oviposition site preferences by *Aedes aegypti*. Proc. Natl. Acad. Sci. USA 105, 9262–9267. [PubMed: 18607006]

Raiser G (2018). SeqPeelSort: a spike sorting algorithm for single sensillum recordings. J. Open Source Softw. 3, 792.

Raji JI, Melo N, Castillo JS, Gonzalez S, Saldana V, Stensmyr MC, and DeGennaro M (2019). *Aedes aegypti* mosquitoes detect acidic volatiles found in human odor using the IR8a pathway. Curr. Biol. 29, 1253–1262.e7. [PubMed: 30930038]

Rharrabe K, Jacquin-Joly E, and Marion-Poll F (2014). Electrophysiological and behavioral responses of *Spodoptera littoralis* caterpillars to attractive and repellent plant volatiles. Front. Ecol. Evol. 2, 5.

Rinker DC, Pitts RJ, Zhou X, Suh E, Rokas A, and Zwiebel LJ (2013). Blood meal-induced changes to antennal transcriptome profiles reveal shifts in odor sensitivities in *Anopheles gambiae*. Proc. Natl. Acad. Sci. USA 110, 8260–8265. [PubMed: 23630291]

Sattler MA, Mtasiwa D, Kiama M, Premji Z, Tanner M, Killeen GF, and Lengeler C (2005). Habitat characterization and spatial distribution of *Anopheles* sp. mosquito larvae in Dar es Salaam (Tanzania) during an extended dry period. Malar. J. 4, 4. [PubMed: 15649333]

Schulz S, and Dickschat JS (2007). Bacterial volatiles: the smell of small organisms. Nat. Prod. Rep. 24, 814–842. [PubMed: 17653361]

Sih A (1986). Antipredator responses and the perception of danger by mosquito larvae. Ecology 67, 434–441.

Silberbush A, Markman S, Lewinsohn E, Bar E, Cohen JE, and Blaustein L (2010). Predator-released hydrocarbons repel oviposition by a mosquito. Ecol. Lett. 13, 1129–1138. [PubMed: 20618841]

Soleimani-Ahmadi M, Vatandoost H, and Zare M (2014). Characterization of larval habitats for anopheline mosquitoes in a malarious area under elimination program in the southeast of Iran. Asian Pac. J. Trop. Biomed. 4 (Suppl 1), S73–S80. [PubMed: 25183151]

Su CY, Menuz K, Reisert J, and Carlson JR (2012). Non-synaptic inhibition between grouped neurons in an olfactory circuit. Nature 492, 66–71. [PubMed: 23172146]

Suh E, Choe DH, Saveer AM, and Zwiebel LJ (2016). Suboptimal larval habitats modulate oviposition of the malaria vector mosquito *Anopheles coluzzii*. PLoS ONE 11, e0149800. 10.1371/journal.pone.0149800. [PubMed: 26900947]

Sun H, Liu F, Ye Z, Baker A, and Zwiebel LJ (2020). Mutagenesis of the orco odorant receptor co-receptor impairs olfactory function in the malaria vector Anopheles coluzzii. Insect Biochem. Mol. Biol. 127, 103497. [PubMed: 33188923]

Task D, Lin C-C, Afify A, Li H, Vulpe A, Menuz K, and Potter CJ (2020). Widespread polymodal chemosensory receptor expression in *Drosophila* olfactory neurons. bioRxiv. 10.1101/2020.11.07.355651.

Tomberlin JK, Crippen TL, Wu G, Griffin AS, Wood TK, and Kilner RM (2017). Indole: An evolutionarily conserved influencer of behavior across kingdoms. BioEssays 39, 1600203.

Turlings TCJ, Tumlinson JH, Heath RR, Proveaux AT, and Doolittle RE (1991). Isolation and identification of allelochemicals that attract the larval parasitoid, *Cotesia marginiventris* (Cresson), to the microhabitat of one of its hosts. J. Chem. Ecol. 17, 2235–2251. [PubMed: 24258602]

Tusting LS, Thwing J, Sinclair D, Fillinger U, Gimnig J, Bonner KE, Bottomley C, and Lindsay SW (2013). Mosquito larval source management for controlling malaria. Cochrane Database Syst. Rev. 2013, CD008923.

Varela C, Siebert T, Cozzolino D, Rose L, McLean H, and Henschke PA (2009). Discovering a chemical basis for differentiating wines made by fermentation with 'wild' indigenous and inoculated yeasts: role of yeast volatile compounds. Aust. J. Grape Wine Res. 15, 238–248.

Waliwitiya R, Kennedy CJ, and Lowenberger CA (2009). Larvicidal and oviposition-altering activity of monoterpenoids, trans-anithole and rosemary oil to the yellow fever mosquito Aedes aegypti (Diptera: Culicidae). Pest Manag. Sci. 65, 241–248. [PubMed: 19086001]

Wang G, Carey AF, Carlson JR, and Zwiebel LJ (2010). Molecular basis of odor coding in the malaria vector mosquito *Anopheles gambiae*. Proc. Natl. Acad. Sci. USA 107, 4418–4423. [PubMed: 20160092]

Wotton RS, Chaloner DT, Yardley CA, and Merritt RW (1997). Growth of *Anopheles* mosquito larvae on dietary microbiota in aquatic surface microlayers. Med. Vet. Entomol. 11, 65–70. [PubMed: 9061679]

Xia Y, Wang G, Buscariollo D, Pitts RJ, Wenger H, and Zwiebel LJ (2008). The molecular and cellular basis of olfactory-driven behavior in *Anopheles gambiae* larvae. Proc. Natl. Acad. Sci. USA 105, 6433–6438. [PubMed: 18427108]

Yang L, Liu Y, Richoux GM, Bernier UR, Linthicum KJ, and Bloomquist JR (2019). Induction coil heating improves the efficiency of insect olfactory studies. Front. Ecol. Evol. 7, 247.

Younger MA, Herre M, Ehrlich AR, Gong Z, Gilbert ZN, Rahiel S, Matthews BJ, and Vosshall LB (2020). Non-canonical odor coding ensures unbreakable mosquito attraction to humans. bioRxiv. 10.1101/2020.11.07.368720.

Zacharuk RY, Yin LR, and Blue SG (1971). Fine structure of the antenna and its sensory cone in larvae of *Aedes aegypti (L.)*. J. Morphol. 135, 273–297. [PubMed: 5126255]

Zwiebel LJ, and Takken W (2004). Olfactory regulation of mosquito-host interactions. Insect Biochem. Mol. Biol. 34, 645–652. [PubMed: 15242705]

Highlights

- Anopheline larvae detect, discriminate, and respond to volatile odors
- The larval sensory cone has a broad response profile
- Responses are linked to discrete neuron groups with distinctive sensitivity profiles
- Larval behavioral responses to volatiles that robustly activate the sensory cone

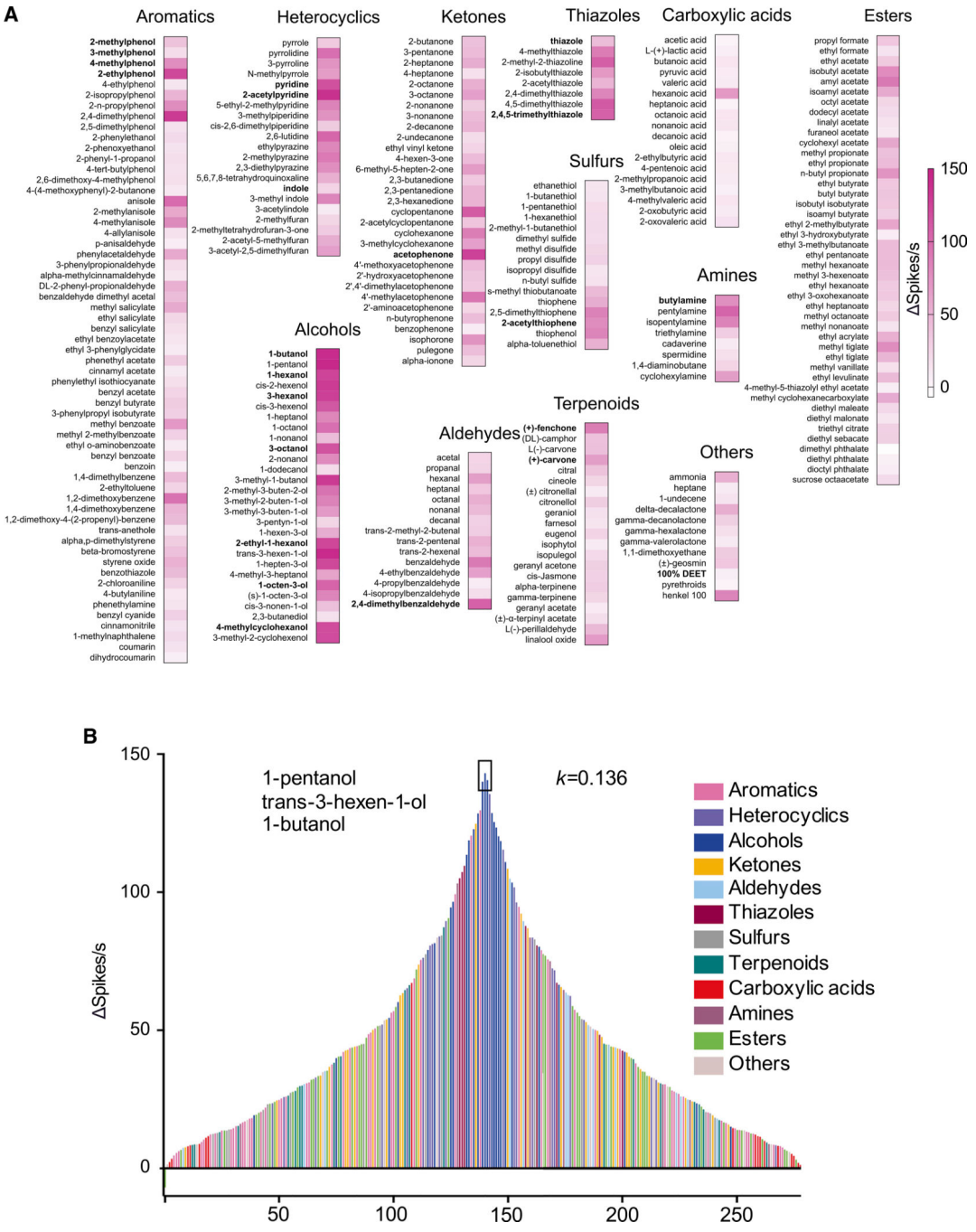

Figure 1. Broad response profiles of the larval sensory cone in *An. Coluzzii*

(A) Response profile of the larval sensory cone to 281 odorants of diverse chemical groups (n = 6) at a 10^{-2} dilution. Odorants highlighted in bold evoke behavioral responses in *An. coluzzii* larvae (Table S1).

(B) Tuning curve reveals the breadth of the larval sensory cone. The 281 odorants are distributed along the x axis according to the strengths of the responses they elicited from the sensory cone. The odors that elicited the strongest responses are near the center of the distribution; those that elicited the weakest responses are near the edges. Negative values

indicate inhibitory responses. Each odorant is color coded based on its chemical class. The kurtosis (k) value, as a statistical measure of “peakedness,” is shown on the right side of the plot.

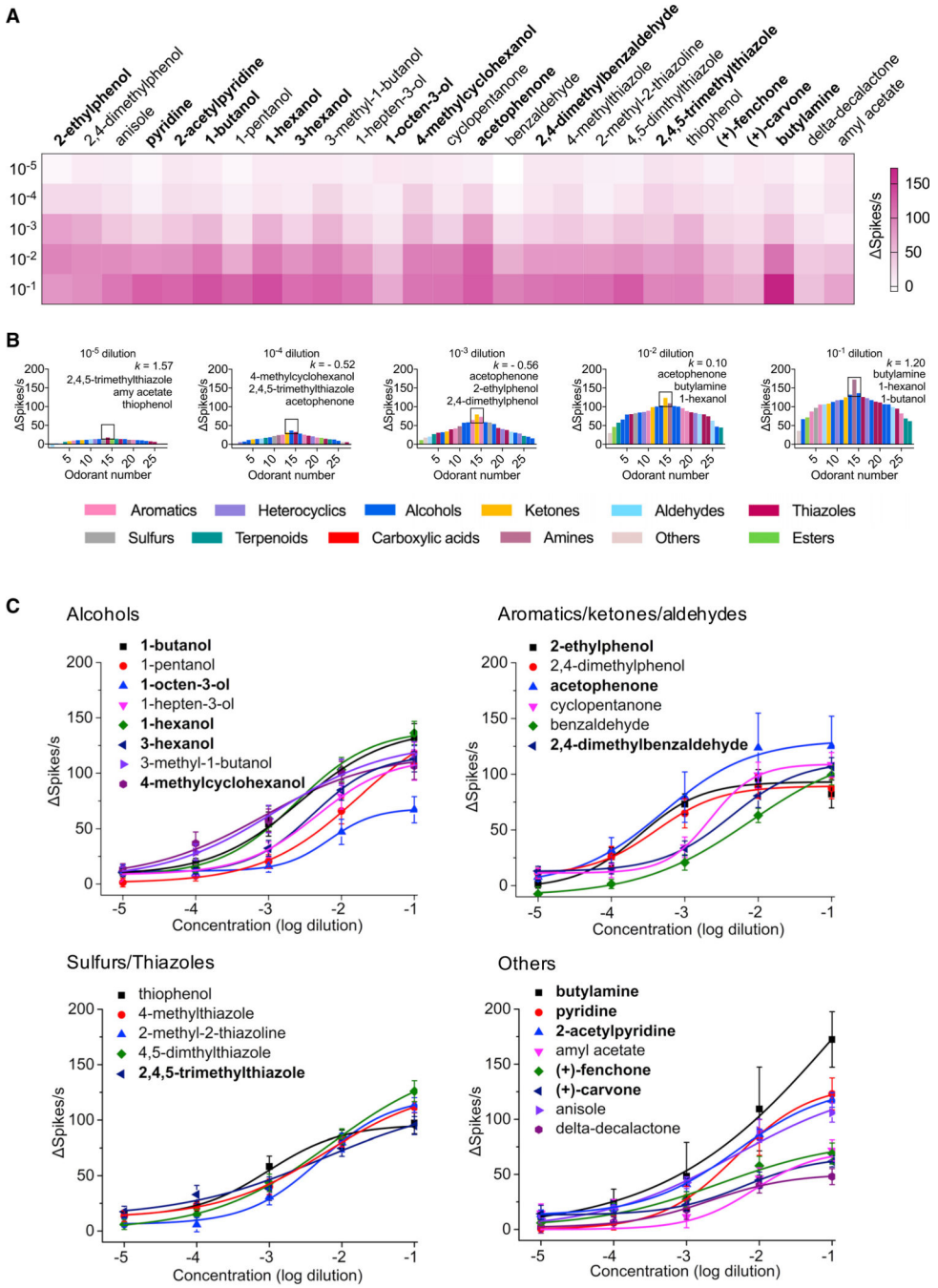

Figure 2. Odor-evoked dose-dependent responses of the larval sensory cone

(A) Dose-dependent response to a panel of 27 odorants displayed along heatmap quadrants. (B) Tuning curves of the larval sensory cone to odorant dilutions across five orders of magnitude. The 27 odorants are distributed along the x axis according to the strength of the responses they elicited from the sensory cone. Each odorant is color coded based on its chemical class. The odorants that elicited the strongest responses are near the center of the distribution; those that elicited the weakest responses are near the edges. The three odorants eliciting the highest firing frequency in the sensory cone are noted for each dilution.

(C) Dose-response curves of the larval sensory cone to these 27 odorant stimuli; n = 6–10 for each odorant dilution. Error bars indicated SEM. Neuronal responses across 0.5-s intervals for all odorant stimuli were calculated by subtracting solvent-alone responses and corrected for background activity.

(A and C) The odorants highlighted in bold evoked behavioral responses in *An. coluzzii* larvae (Table S1).

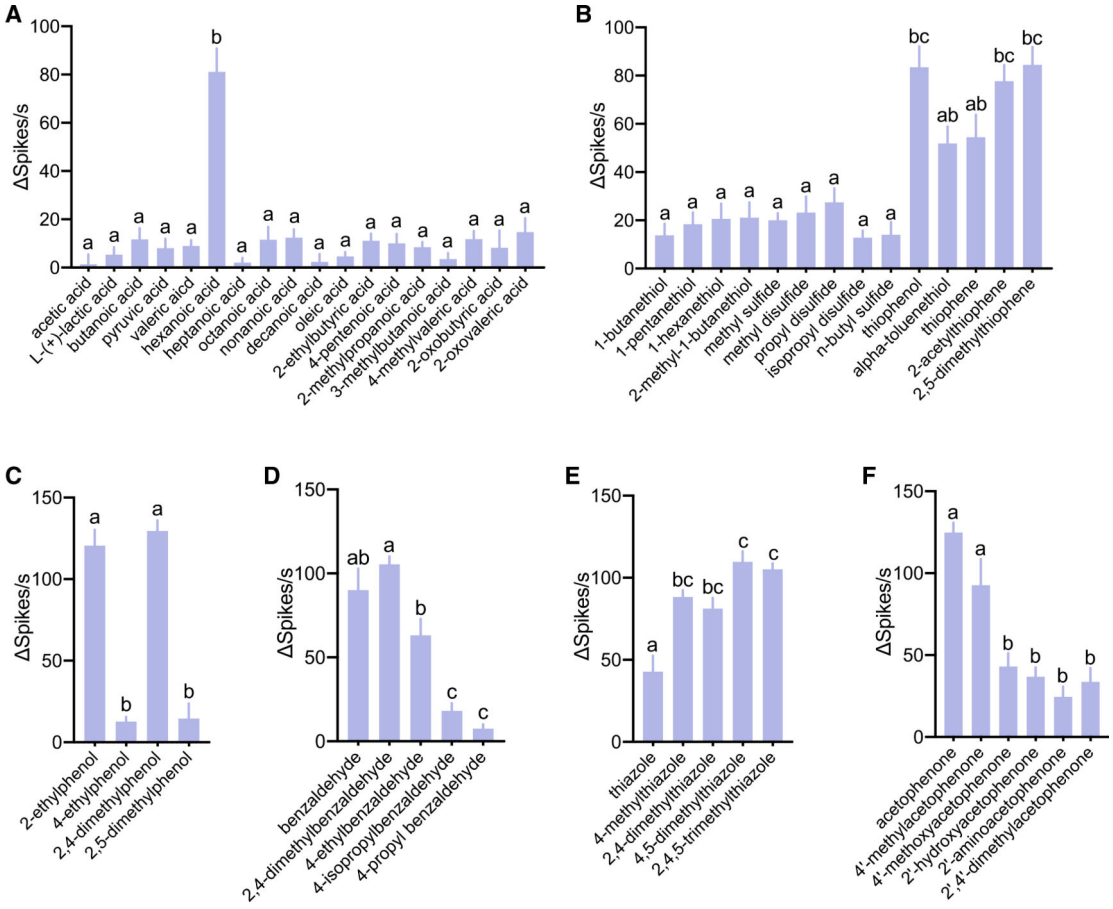

Figure 3. Responses of larval sensory cone to odorants with similar structures (n = 6)

(A–F) Responses of larval sensory cone to: (A) aliphatic carboxylic acids; (B) aliphatic and aromatic sulfurs; (C) ethylphenol-derived compounds; (D) benzaldehyde-derived compounds; (E) thiazole-derived compounds with increased alkane branches in the heterocyclic ring; and (F) acetophenone-derived compounds. Error bars indicate SEM. One-way ANOVA Tukey's test was applied in the statistical analysis, with $p < 0.05$ indicating a significant difference. Different letters (a, b, c) indicate significant statistical differences ($p < 0.05$); those with the same letters are not statistically distinct.

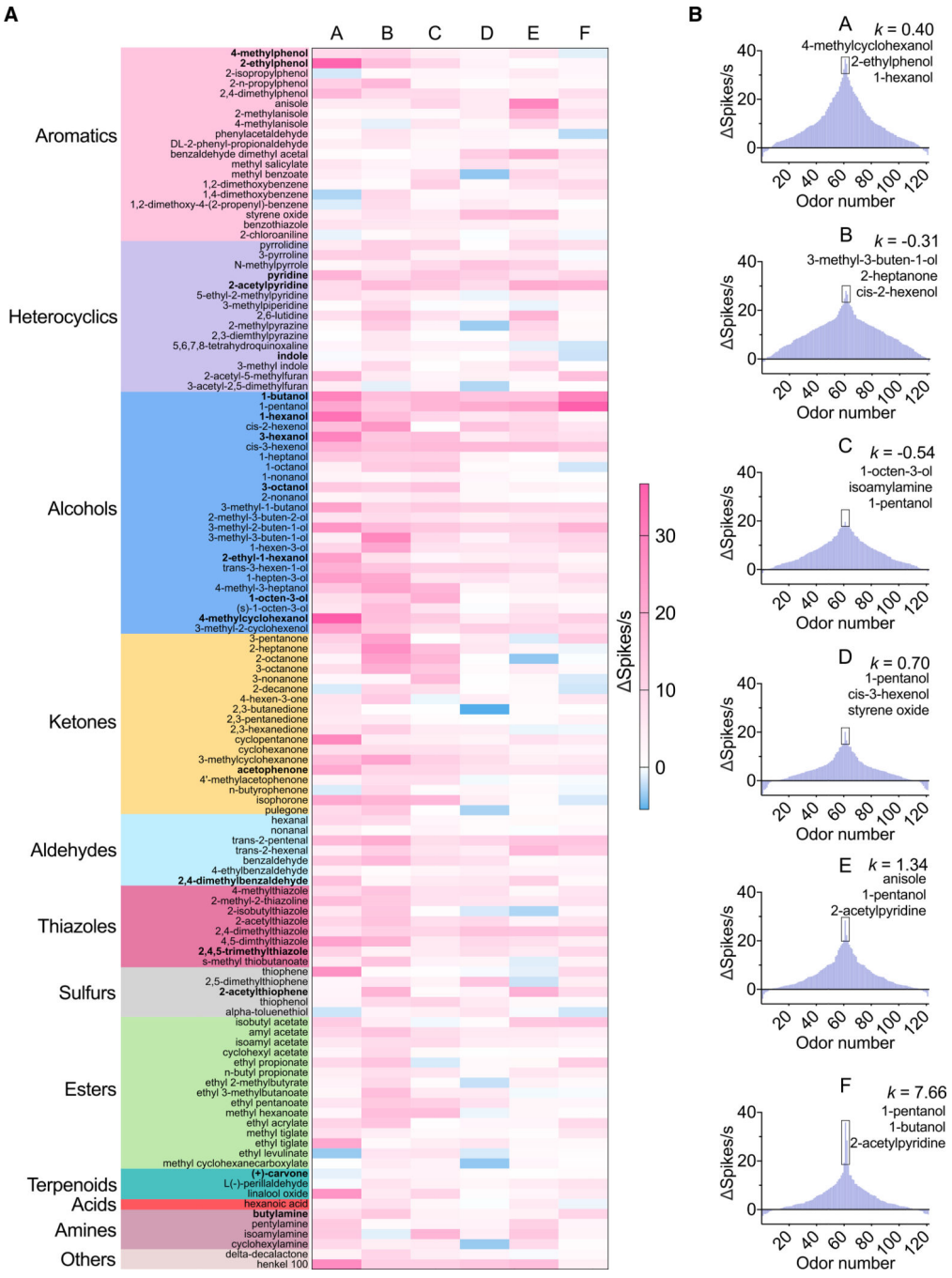

Figure 4. Response profiles across neuron groups to 121 odorants in the sensory cone (n = 3–5)

Neuronal responses for all odorant stimuli at 10^{-2} dilution were calculated by subtracting solvent-alone responses and corrected for background activity. Thereafter, spike units were sorted using a custom-designed SSSort software algorithm (see STAR Methods).

(A) Heatmap of response profile of six neuron groups (A–F) to 121 odorants; the odorants highlighted in bold evoked behavioral responses in *An. coluzzii* larvae (Table S1). Each odorant is color coded based on its chemical class.

(B) Tuning curves of the sorted six neuron groups (A–F) in response to 121 odorants. The corresponding kurtosis (k) values were calculated for each neuron group. The top three odorants contributing to the peak response are listed.

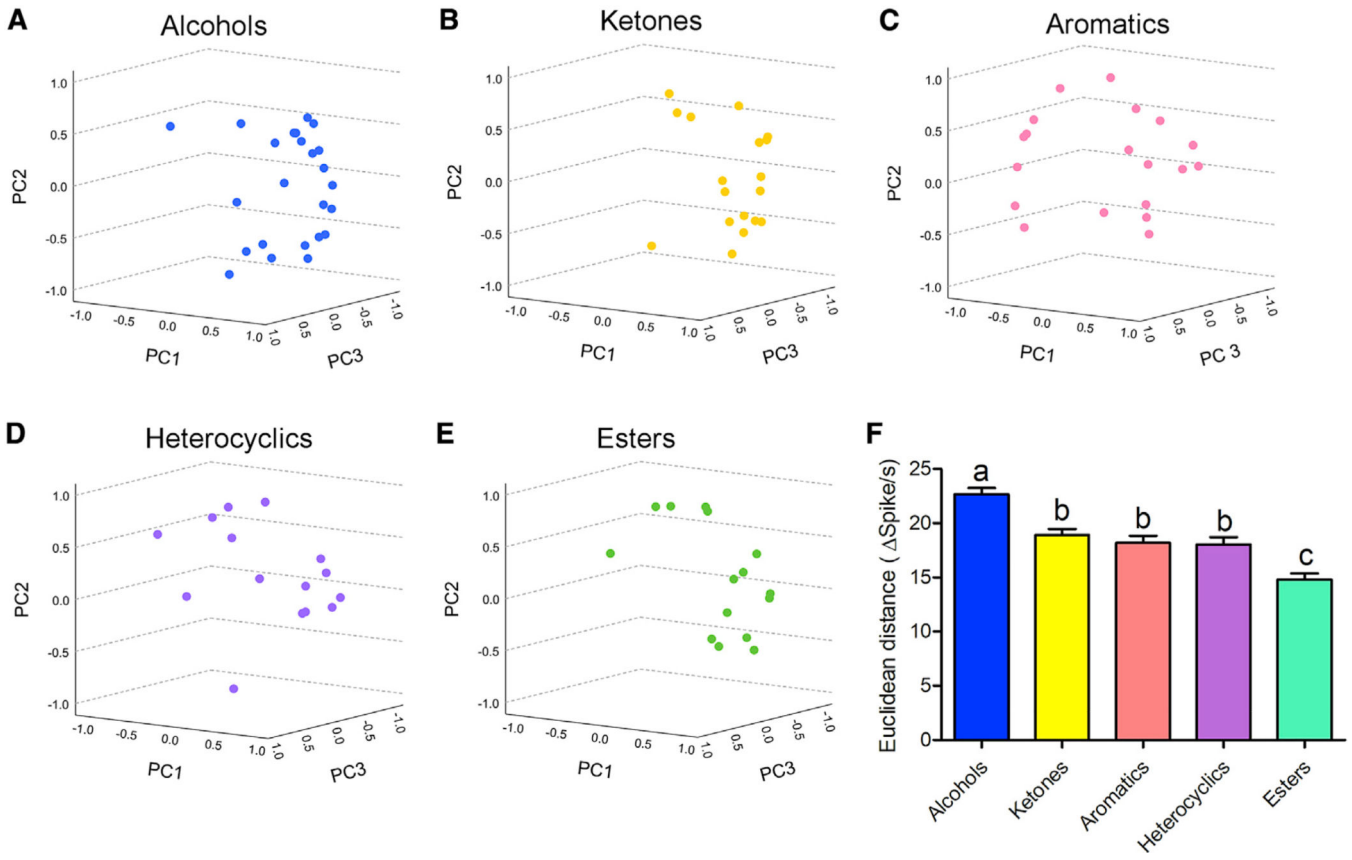

Figure 5. Five major chemical classes constitute the odor space of the larval sensory cone

(A–E) Three-dimensional presentation of responses to (A) alcohols, (B) ketones, (C) aromatics, (D) heterocyclics, and (E) esters distributed across the odor space of the larval sensory cone. Each odorant is color coded based on its chemical class. Principal-component analysis (PCA) was conducted using IBM SPSS Statistics, and Euclidean distance between each chemical pair was calculated.

(F) Mean Euclidean distance of each chemical class in the odor space. Error bars indicate SEM. One-way ANOVA (non-parametric Kruskal-Wallis test) was conducted to determine the significant differences among chemical classes. Different letters (a, b, c) indicate significant statistical differences ($p < 0.05$); those with the same letters are not statistically distinct.

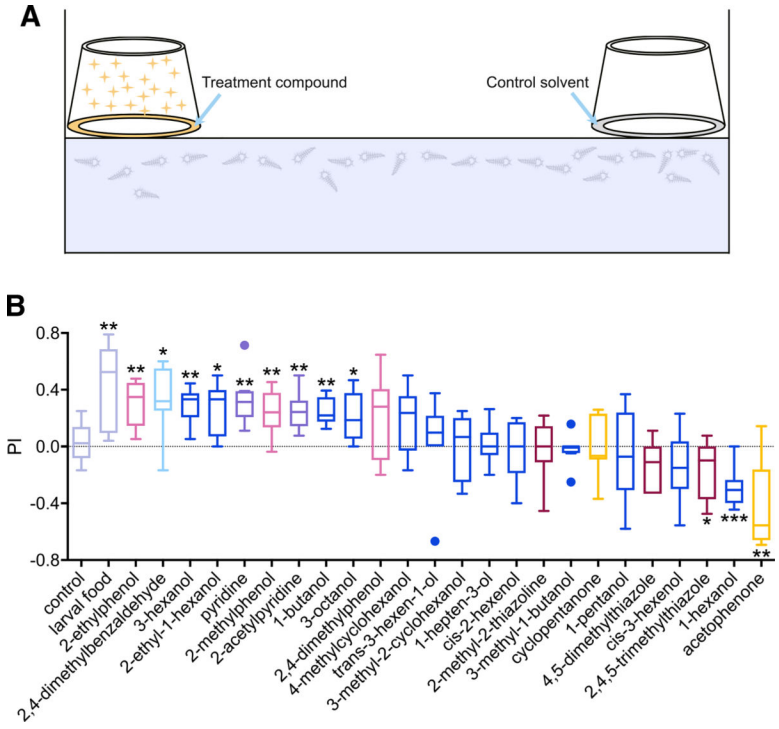

Figure 6. Behavioral responses of anopheline larvae to volatiles

(A) Schematic of the behavioral assay.

(B) Boxplot of preference index (n = 7–10) of mosquito larvae responses to larval food volatiles, as well as 24 unitary odorant volatiles and solvent-alone controls. Respective PI values for each compound were compared with that of solvent-alone sham assays and assessed for statistical significance using unpaired, two-tailed Student's t tests with Welch's correction. Error bars indicate SEM. Significant differences are defined as *p < 0.05 and **p < 0.01. Each odorant is color coded based on its chemical class, shown in Figure 1B.

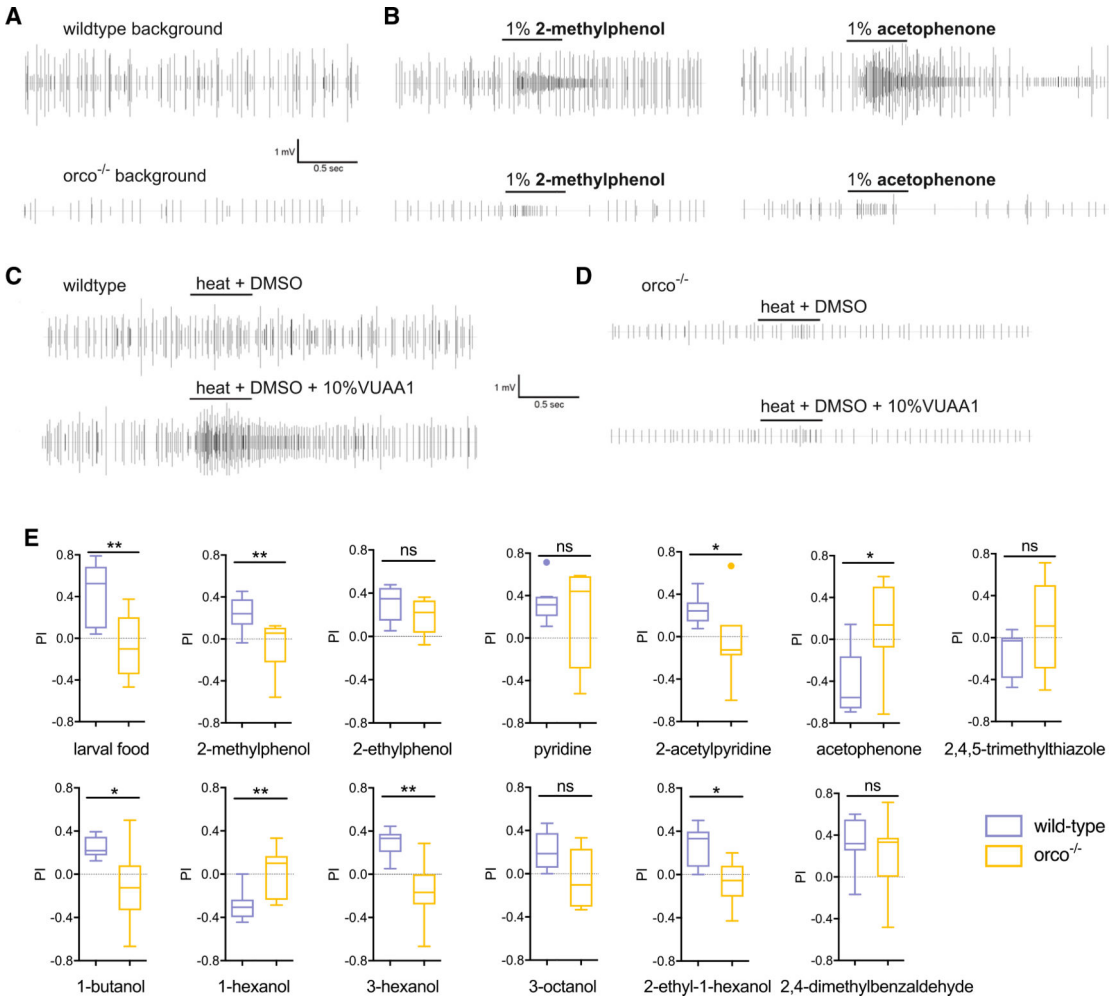

Figure 7. Neuronal and behavioral responses to volatiles are Orco-mediated in mosquito larvae

(A) Representative raw spike recording of background electrophysiological activity in the larval antennal sensory cone of wild-type and *orco*$^{-/-}$ mosquitoes.

(B) Representative spike recording of electrophysiological responses of larval antennal sensory cone to 2-methylphenol and acetophenone in wild-type and *orco*$^{-/-}$ mosquitoes.

(C) Representative signal trace of electrophysiological responses of larval antennal sensory cone to the Orco agonist VUAA1 in wild-type mosquitoes.

(D) Representative signal trace of electrophysiological responses of larval antennal sensory cone to the Orco agonist VUAA1 in *orco*$^{-/-}$ mosquitoes.

(E) Comparison of behavioral responses of wild-type and *orco*$^{-/-}$ mosquito larvae to larval food and 12 odorants (n = 7–10). Error bars indicate SEM. Significant differences are defined as *p < 0.05 and **p < 0.01 in the unpaired t test with Welch's correction. ns, no significant difference.

KEY RESOURCES TABLE

REAGENT or RESOURCE	SOURCE	IDENTIFIER
Chemicals, peptides, and recombinant proteins		
2-methylphenol	Sigma Aldrich	CAS# 95-48-7
3-methylphenol	Sigma Aldrich	CAS# 108-39-4
4-methylphenol	Sigma Aldrich	CAS# 106-44-5
2-ethylphenol	Sigma Aldrich	CAS# 90-00-6
4-ethylphenol	Sigma Aldrich	CAS# 123-07-9
2-isopropylphenol	Sigma Aldrich	CAS# 88-69-7
2-n-propylphenol	Sigma Aldrich	CAS# 644-35-9
2,4-dimethylphenol	Sigma Aldrich	CAS# 105-67-9
2,5-dimethylphenol	Sigma Aldrich	CAS# 95-87-4
2-phenylethanol	Sigma Aldrich	CAS# 60-12-8
2-phenoxyethanol	Sigma Aldrich	CAS# 122-99-6
2-phenyl-1-propanol	Sigma Aldrich	CAS# 1123-85-9
4-tert-butylphenol	Sigma Aldrich	CAS# 98-54-4
2,6-dimethoxy-4-methylphenol	Sigma Aldrich	CAS# 6638-05-7
4-(4-methoxyphenyl)-2-butanone	Sigma Aldrich	CAS# 104-20-1
anisole	Sigma Aldrich	CAS# 100-66-3
2-methylanisole	Sigma Aldrich	CAS# 578-58-5
4-methylanisole	Sigma Aldrich	CAS# 104-93-8
4-allylanisole	Sigma Aldrich	CAS# 140-67-0
p-anisaldehyde	Sigma Aldrich	CAS# 123-11-5
phenylacetaldehyde	Sigma Aldrich	CAS# 122-78-1
3-phenylpropionaldehyde	Sigma Aldrich	CAS# 104-53-0
alpha-methylcinnamaldehyde	Sigma Aldrich	CAS# 101-39-3
DL-2-phenyl-propionaldehyde	Sigma Aldrich	CAS# 93-53-8
benzaldehyde dimethyl acetal	Sigma Aldrich	CAS# 1125-88-8
methyl salicylate	Sigma Aldrich	CAS# 119-36-8
ethyl salicylate	Sigma Aldrich	CAS# 118-61-6
benzyl salicylate	Sigma Aldrich	CAS# 118-58-1
ethyl benzoylacetate	Sigma Aldrich	CAS# 94-02-0
ethyl 3-phenylglycidate	Sigma Aldrich	CAS# 121-39-1
phenethyl acetate	Sigma Aldrich	CAS# 103-45-7
cinnamyl acetate	Sigma Aldrich	CAS# 103-54-8
phenylethyl isothiocyanate	Sigma Aldrich	CAS# 2257-09-2
benzyl acetate	Sigma Aldrich	CAS# 140-11-4
benzyl butyrate	Sigma Aldrich	CAS# 103-37-7
3-phenylpropyl isobutyrate	Sigma Aldrich	CAS# 103-58-2
methyl benzoate	Sigma Aldrich	CAS# 93-58-3
methyl 2-methylbenzoate	Sigma Aldrich	CAS# 89-71-4

REAGENT or RESOURCE	SOURCE	IDENTIFIER
ethyl o-aminobenzoate	Sigma Aldrich	CAS# 87-25-2
benzyl benzoate	Sigma Aldrich	CAS# 120-51-4
benzoin	Sigma Aldrich	CAS# 119-53-9
1,4-dimethylbenzene	Sigma Aldrich	CAS# 106-42-3
2-ethyltoluene	Sigma Aldrich	CAS# 611-14-3
1,2-dimethoxybenzene	Sigma Aldrich	CAS# 91-16-7
1,4-dimethoxybenzene	Sigma Aldrich	CAS# 150-78-7
1,2-dimethoxy-4-(2-propenyl)-benzene	Sigma Aldrich	CAS# 93-15-2
trans-anethole	Sigma Aldrich	CAS# 4180-23-8
alpha,p-dimethylstyrene	Sigma Aldrich	CAS# 1195-32-0
beta-bromostyrene	Sigma Aldrich	CAS# 103-64-0
styrene oxide	Sigma Aldrich	CAS# 96-09-3
benzothiazole	Sigma Aldrich	CAS# 95-16-9
2-chloroaniline	Sigma Aldrich	CAS# 95-51-2
4-butylaniline	Sigma Aldrich	CAS# 104-13-2
phenethylamine	Sigma Aldrich	CAS# 64-04-0
benzyl cyanide	Sigma Aldrich	CAS# 140-29-4
cinnamonitrile	Sigma Aldrich	CAS# 1885-38-7
1-methylnaphthalene	Sigma Aldrich	CAS# 90-12-0
coumarin	Sigma Aldrich	CAS# 91-64-5
dihydrocoumarin	Sigma Aldrich	CAS# 119-84-6
pyrrole	Sigma Aldrich	CAS# 109-97-7
pyrrolidine	Sigma Aldrich	CAS# 123-75-1
3-pyrroline	Sigma Aldrich	CAS# 109-96-6
N-methylpyrrole	Sigma Aldrich	CAS# 96-54-8
pyridine	Sigma Aldrich	CAS# 110-86-1
2-acetylpyridine	Sigma Aldrich	CAS# 1122-62-9
5-ethyl-2-methylpyridine	Sigma Aldrich	CAS# 104-90-5
3-methylpiperidine	Sigma Aldrich	CAS# 626-56-2
cis-2,6-dimethylpiperidine	Sigma Aldrich	CAS# 766-17-6
2,6-lutidine	Sigma Aldrich	CAS# 108-48-5
ethylpyrazine	Sigma Aldrich	CAS# 3925-00-3
2-methylpyrazine	Sigma Aldrich	CAS# 109-08-0
2,3-diethylpyrazine	Sigma Aldrich	CAS# 5707-24-1
5,6,7,8-tetrahydroquinoxaline	Sigma Aldrich	CAS# 34413-35-9
indole	Sigma Aldrich	CAS# 120-72-9
3-methyl indole	Sigma Aldrich	CAS# 83-34-1
3-acetylindole	Sigma Aldrich	CAS# 703-80-0
2-methylfuran	Sigma Aldrich	CAS# 534-22-5
2-methyltetrahydrofuran-3-one	Sigma Aldrich	CAS# 3188-00-9
2-acetyl-5-methylfuran	Sigma Aldrich	CAS# 1193-79-9
3-acetyl-2,5-dimethylfuran	Sigma Aldrich	CAS# 10599-70-9

REAGENT or RESOURCE	SOURCE	IDENTIFIER
1-butanol	Sigma Aldrich	CAS# 71-36-3
1-pentanol	Sigma Aldrich	CAS# 71-41-0
1-hexanol	Sigma Aldrich	CAS# 111-27-3
cis-2-hexenol	Sigma Aldrich	CAS# 928-94-9
3-hexanol	Sigma Aldrich	CAS# 623-37-0
cis-3-hexenol	Sigma Aldrich	CAS# 928-96-1
1-heptanol	Sigma Aldrich	CAS# 111-70-6
1-octanol	Sigma Aldrich	CAS# 111-87-5
1-nonanol	Sigma Aldrich	CAS# 143-08-8
3-octanol	Sigma Aldrich	CAS# 589-98-0
2-nonanol	Sigma Aldrich	CAS# 628-99-9
1-dodecanol	Sigma Aldrich	CAS# 112-53-8
3-methyl-1-butanol	Sigma Aldrich	CAS# 123-51-3
2-methyl-3-buten-2-ol	Sigma Aldrich	CAS# 115-18-4
3-methyl-2-buten-1-ol	Sigma Aldrich	CAS# 556-82-1
3-methyl-3-buten-1-ol	Sigma Aldrich	CAS# 763-32-6
3-pentyn-1-ol	Sigma Aldrich	CAS# 10229-10-4
1-hexen-3-ol	Sigma Aldrich	CAS# 4798-44-1
2-ethyl-1-hexanol	Sigma Aldrich	CAS# 104-76-7
trans-3-hexen-1-ol	Sigma Aldrich	CAS# 928-97-2
1-hepten-3-ol	Sigma Aldrich	CAS# 4938-52-7
4-methyl-3-heptanol	Sigma Aldrich	CAS# 14979-39-6
1-octen-3-ol	Sigma Aldrich	CAS# 3391-86-4
(s)-1-octen-3-ol	Sigma Aldrich	CAS# 24587-53-9
cis-3-nonen-1-ol	Sigma Aldrich	CAS# 10340-23-5
2,3-butanediol	Sigma Aldrich	CAS# 513-85-9
4-methylcyclohexanol	Sigma Aldrich	CAS# 589-91-3
3-methyl-2-cyclohexenol	Sigma Aldrich	CAS# 21378-21-2
2-butanone	Sigma Aldrich	CAS# 78-93-3
3-pentanone	Sigma Aldrich	CAS# 96-22-0
2-heptanone	Sigma Aldrich	CAS# 110-43-0
4-heptanone	Sigma Aldrich	CAS# 123-19-3
2-octanone	Sigma Aldrich	CAS# 111-13-7
3-octanone	Sigma Aldrich	CAS# 106-68-3
2-nonanone	Sigma Aldrich	CAS# 821-55-6
3-nonanone	Sigma Aldrich	CAS# 925-78-0
2-decanone	Sigma Aldrich	CAS# 693-54-9
2-undecanone	Sigma Aldrich	CAS# 112-12-9
ethyl vinyl ketone	Sigma Aldrich	CAS# 1629-58-9
4-hexen-3-one	Sigma Aldrich	CAS# 2497-21-4
6-methyl-5-hepten-2-one	Sigma Aldrich	CAS# 110-93-0
2,3-butanedione	Sigma Aldrich	CAS# 431-03-8

REAGENT or RESOURCE	SOURCE	IDENTIFIER
2,3-pentanedione	Sigma Aldrich	CAS# 600-14-6
2,3-hexanedione	Sigma Aldrich	CAS# 3848-24-6
cyclopentanone	Sigma Aldrich	CAS# 120-92-3
2-acetylcyclopentanone	Sigma Aldrich	CAS# 1670-46-8
cyclohexanone	Sigma Aldrich	CAS# 108-94-1
3-methylcyclohexanone	Sigma Aldrich	CAS# 591-24-2
acetophenone	Sigma Aldrich	CAS# 98-86-2
4′-methoxyacetophenone	Sigma Aldrich	CAS# 100-06-1
2′-hydroxyacetophenone	Sigma Aldrich	CAS# 118-93-4
2′,4’-dimethylacetophenone	Sigma Aldrich	CAS# 89-74-7
4’-methylacetophenone	Sigma Aldrich	CAS# 122-00-9
2′-aminoacetophenone	Sigma Aldrich	CAS# 551-93-9
n-butyrophenone	Sigma Aldrich	CAS# 495-40-9
benzophenone	Sigma Aldrich	CAS# 119-61-9
Isophorone	Sigma Aldrich	CAS# 78-59-1
pulegone	Sigma Aldrich	CAS# 89-82-7
alpha-ionone	Sigma Aldrich	CAS# 127-41-3
acetal	Sigma Aldrich	CAS# 105-57-7
propanal	Sigma Aldrich	CAS# 123-38-6
hexanal	Sigma Aldrich	CAS# 66-25-1
heptanal	Sigma Aldrich	CAS# 111-71-7
octanal	Sigma Aldrich	CAS# 124-13-0
nonanal	Sigma Aldrich	CAS# 124-19-6
decanal	Sigma Aldrich	CAS# 112-31-2
trans-2-methyl-2-butenal	Sigma Aldrich	CAS# 497-03-0
trans-2-pentenal	Sigma Aldrich	CAS# 1576-87-0
trans-2-hexenal	Sigma Aldrich	CAS# 6728-26-3
benzaldehyde	Sigma Aldrich	CAS# 100-52-7
4-ethylbenzaldehyde	Sigma Aldrich	CAS# 4748-78-1
4-propylbenzaldehyde	Sigma Aldrich	CAS# 28785-06-0
4-isopropylbenzaldehyde	Sigma Aldrich	CAS# 122-03-2
2,4-dimethylbenzaldehyde	Sigma Aldrich	CAS# 15764-16-6
thiazole	Sigma Aldrich	CAS# 288-47-1
4-methylthiazole	Sigma Aldrich	CAS# 693-95-8
2-methyl-2-thiazoline	Sigma Aldrich	CAS# 2346-00-1
2-isobutylthiazole	Sigma Aldrich	CAS# 18640-74-9
2-acetylthiazole	Sigma Aldrich	CAS# 24295-03-2
2,4-dimethylthiazole	Sigma Aldrich	CAS# 541-58-2
4,5-dimethylthiazole	Sigma Aldrich	CAS# 3581-91-7
2,4,5-trimethylthiazole	Sigma Aldrich	CAS# 13623-11-5
ethanethiol	Sigma Aldrich	CAS# 75-08-1
1-butanethiol	Sigma Aldrich	CAS# 109-79-5

REAGENT or RESOURCE	SOURCE	IDENTIFIER
1-pentanethiol	Sigma Aldrich	CAS# 110-66-7
1-hexanethiol	Sigma Aldrich	CAS# 111-31-9
2-methyl-1-butanethiol	Sigma Aldrich	CAS# 1878-18-8
dimethyl sulfide	Sigma Aldrich	CAS# 75-18-3
methyl disulfide	Sigma Aldrich	CAS# 624-92-0
propyl disulfide	Sigma Aldrich	CAS# 629-19-6
isopropyl disulfide	Sigma Aldrich	CAS# 4253-89-8
n-butyl sulfide	Sigma Aldrich	CAS# 544-40-1
s-methyl thiobutanoate	Sigma Aldrich	CAS# 2432-51-1
thiophene	Sigma Aldrich	CAS# 110-02-1
2,5-dimethylthiophene	Sigma Aldrich	CAS# 638-02-8
2-acetylthiophene	Sigma Aldrich	CAS# 88-15-3
thiophenol	Sigma Aldrich	CAS# 108-98-5
alpha-toluenethiol	Sigma Aldrich	CAS# 100-53-8
(+)-fenchone	Sigma Aldrich	CAS# 4695-62-9
(DL)-camphor	Sigma Aldrich	CAS# 76-22-2
L(−)-carvone	Sigma Aldrich	CAS# 6485-40-1
(+)-carvone	Sigma Aldrich	CAS# 2244-16-8
citral	Sigma Aldrich	CAS# 5392-40-5
cineole	Sigma Aldrich	CAS# 470-82-6
(±) citronellal	Sigma Aldrich	CAS# 106-23-0
citronellol	Sigma Aldrich	CAS# 106-22-9
geraniol	Sigma Aldrich	CAS# 106-24-1
farnesol	Sigma Aldrich	CAS# 4602-84-0
eugenol	Sigma Aldrich	CAS# 97-53-0
isophytol	Sigma Aldrich	CAS# 505-32-8
isopulegol	Sigma Aldrich	CAS# 7786-67-6
geranyl acetone	Sigma Aldrich	CAS# 3796-70-1
cis-Jasmone	Sigma Aldrich	CAS# 488-10-8
alpha-terpinene	Sigma Aldrich	CAS# 99-86-5
gamma-terpinene	Sigma Aldrich	CAS# 99-85-4
geranyl acetate	Sigma Aldrich	CAS# 105-87-3
(±)-α-terpinyl acetate	Sigma Aldrich	CAS# 80-26-2
L(−)-perillaldehyde	Sigma Aldrich	CAS# 18031-40-8
linalool oxide	Sigma Aldrich	CAS# 60047-17-8
acetic acid	Sigma Aldrich	CAS# 64-19-7
L-(+)-lactic acid	Sigma Aldrich	CAS# 79-33-4
butanoic acid	Sigma Aldrich	CAS# 107-92-6
pyruvic acid	Sigma Aldrich	CAS# 127-17-3
valeric acid	Sigma Aldrich	CAS# 109-52-4
hexanoic acid	Sigma Aldrich	CAS# 142-62-1
heptanoic acid	Sigma Aldrich	CAS# 111-14-8

REAGENT or RESOURCE	SOURCE	IDENTIFIER
octanoic acid	Sigma Aldrich	CAS# 124-07-2
nonanoic acid	Sigma Aldrich	CAS# 112-05-0
decanoic acid	Sigma Aldrich	CAS# 334-48-5
oleic acid	Sigma Aldrich	CAS# 112-80-1
2-ethylbutyric acid	Sigma Aldrich	CAS# 88-09-5
4-pentenoic acid	Sigma Aldrich	CAS# 591-80-0
2-methylpropanoic acid	Sigma Aldrich	CAS# 79-31-2
3-methylbutanoic acid	Sigma Aldrich	CAS# 503-74-2
4-methylvaleric acid	Sigma Aldrich	CAS# 646-07-1
2-oxobutyric acid	Sigma Aldrich	CAS# 600-18-0
2-oxovaleric acid	Sigma Aldrich	CAS# 1821-02-9
propyl formate	Sigma Aldrich	CAS# 110-74-7
ethyl formate	Sigma Aldrich	CAS# 109-94-4
ethyl acetate	Sigma Aldrich	CAS# 141-78-6
isobutyl acetate	Sigma Aldrich	CAS#110-19-0
amyl acetate	Sigma Aldrich	CAS# 628-63-7
isoamyl acetate	Sigma Aldrich	CAS# 123-92-2
octyl acetate	Sigma Aldrich	CAS# 112-14-1
dodecyl acetate	Sigma Aldrich	CAS# 112-66-3
linalyl acetate	Sigma Aldrich	CAS# 115-95-7
furaneol acetate	Sigma Aldrich	CAS# 4166-20-5
cyclohexyl acetate	Sigma Aldrich	CAS# 622-45-7
methyl propionate	Sigma Aldrich	CAS# 554-12-1
ethyl propionate	Sigma Aldrich	CAS# 105-37-3
n-butyl propionate	Sigma Aldrich	CAS# 590-01-2
ethyl butyrate	Sigma Aldrich	CAS# 105-54-4
butyl butyrate	Sigma Aldrich	CAS# 109-21-7
isobutyl isobutyrate	Sigma Aldrich	CAS# 97-85-8
isoamyl butyrate	Sigma Aldrich	CAS# 106-27-4
ethyl 2-methylbutyrate	Sigma Aldrich	CAS# 7452-79-1
ethyl 3-hydroxybutyrate	Sigma Aldrich	CAS# 5405-41-4
ethyl 3-methylbutanoate	Sigma Aldrich	CAS# 108-64-5
ethyl pentanoate	Sigma Aldrich	CAS# 539-82-2
methyl hexanoate	Sigma Aldrich	CAS# 106-70-7
methyl 3-hexenoate	Sigma Aldrich	CAS# 2396-78-3
ethyl hexanoate	Sigma Aldrich	CAS# 123-66-0
ethyl 3-oxohexanoate	Sigma Aldrich	CAS# 3249-68-1
ethyl heptanoate	Sigma Aldrich	CAS# 106-30-9
methyl octanoate	Sigma Aldrich	CAS# 111-11-5
methyl nonanoate	Sigma Aldrich	CAS# 1731-84-6
ethyl acrylate	Sigma Aldrich	CAS# 140-88-5
methyl tiglate	Sigma Aldrich	CAS# 6622-76-0

REAGENT or RESOURCE	SOURCE	IDENTIFIER
ethyl tiglate	Sigma Aldrich	CAS# 5837-78-5
methyl vanillate	Sigma Aldrich	CAS# 3943-74-6
ethyl levulinate	Sigma Aldrich	CAS# 539-88-8
4-methyl-5-thiazolyl ethyl acetate	Sigma Aldrich	CAS# 656-53-1
methyl cyclohexanecarboxylate	Sigma Aldrich	CAS# 4630-82-4
diethyl maleate	Sigma Aldrich	CAS# 141-05-9
diethyl malonate	Sigma Aldrich	CAS# 105-53-3
triethyl citrate	Sigma Aldrich	CAS# 77-93-0
diethyl sebacate	Sigma Aldrich	CAS# 110-40-7
dimethyl phthalate	Sigma Aldrich	CAS# 131-11-3
diethyl phthalate	Sigma Aldrich	CAS# 84-66-2
dioctyl phthalate	Sigma Aldrich	CAS# 117-81-7
sucrose octaacetate	Sigma Aldrich	CAS# 126-14-7
butylamine	Sigma Aldrich	CAS# 109-73-9
pentylamine	Sigma Aldrich	CAS# 110-58-7
isopentylamine	Sigma Aldrich	CAS# 107-85-7
triethylamine	Sigma Aldrich	CAS# 121-44-8
cadaverine	Sigma Aldrich	CAS# 462-94-2
spermidine	Sigma Aldrich	CAS# 124-20-9
1,4-diaminobutane	Sigma Aldrich	CAS# 110-60-1
cyclohexylamine	Sigma Aldrich	CAS# 108-91-8
ammonia	Sigma Aldrich	CAS# 1336-21-6
heptane	Sigma Aldrich	CAS# 142-82-5
1-undecene	Sigma Aldrich	CAS# 821-95-4
delta-decalactone	Sigma Aldrich	CAS# 705-86-2
gamma-decanolactone	Sigma Aldrich	CAS# 706-14-9
gamma-hexalactone	Sigma Aldrich	CAS# 695-06-7
gamma-valerolactone	Sigma Aldrich	CAS# 108-29-2
1,1-dimethoxyethane	Sigma Aldrich	CAS# 534-15-6
(±)-geosmin	Sigma Aldrich	CAS# 16423-19-1
100% DEET	Sigma Aldrich	CAS# 134-62-3
pyrethroids	Sigma Aldrich	MDL# MFCD06202228
VUAA1	Sigma Aldrich	CAS# 525582-84-7
Experimental models: Organisms/strains		
Anopheles coluzzii	BEI Resources	MRA-765
Anopheles coluzzii Orco $^{-/-}$ strain	Zwiebel lab, Vanderbilt University	LJZOrcoKO1
Software and algorithms		

REAGENT or RESOURCE	SOURCE	IDENTIFIER
GraphPad Prism 8	GraphPad	https://www.graphpad.com/scientific-software/prism/
SingleSensillumSort	N/A	https://github.com/grg2rsr/SSSort